POLITECNICO DI TORINO
Repository ISTITUZIONALE

The Renaissance of fullerenes with perovskite solar cells

Original
The Renaissance of fullerenes with perovskite solar cells / Gatti, T., Menna, E., Meneghetti, M., Maggini, M., Petrozza, A., Lamberti, F.. - In: NANO ENERGY. - ISSN 2211-2855. - 41:(2017), pp. 84-100. [10.1016/j.nanoen.2017.09.016]

Availability:
This version is available at: 11583/2977494 since: 2023-03-27T14:26:25Z

Publisher:
Elsevier

Published
DOI:10.1016/j.nanoen.2017.09.016

Terms of use:

This article is made available under terms and conditions as specified in the corresponding bibliographic description in the repository

Publisher copyright

(Article begins on next page)

07 November 2026

The Renaissance of fullerenes with perovskite solar cells

Teresa Gatti[a,*], Enzo Menna[a], Moreno Meneghetti[a], Michele Maggini[a], Annamaria Petrozza[b] Francesco Lamberti[a,*]

[a] *Department of Chemistry, University of Padova, Via Marzolo 1, Padova 35131, Italy*

[b] *Center for NanoScience and Technology @PoliMI, Istituto Italiano di Tecnologia, Via Giovanni Pascoli 70/3, 20133 Milano, Italy.*

*Corresponding authors.

E-mail addresses: teresa.gatti@unipd.it (T. Gatti); francesco.lamberti@dei.unipd.it (F. Lamberti);

Keywords: perovskite solar cell, fullerene, C60, PCBM, electron transporting layer, cross-linked fullerene

Abstract

Fullerenes have been extensively used for more than two decades for the development of organic photovoltaics (OPV). While OPV seems to be a technology almost ready for the market, in the last few years fullerenes are attracting a big interest for the improvement they afford on the already well-performing perovskite solar cells (PSCs). Thanks to PSC integration, interest in fullerenes is rising again, opening up new exciting perspectives for photovoltaics. This review article aims at analyzing the landmark contributions that gave birth to the novel application of fullerenes in PSCs and to the technological solutions that are emerging with them.

1. Introduction

Within the last decade a continuous attention has been addressed to perovskite (PVK) semiconductors as active materials in third generation hybrid organic-inorganic solid state devices [1]. The evolution history of PVK started from the organic-inorganic hybrid lead halide PVK (methylammonium lead iodide, MAPI) [2] and evolved to the most recent organic-inorganic hybrid mixed cations/anions PVK (formamidinium lead iodide/bromide, $FAPbI_3$/$FAPbBr_3$) and to the fully inorganic perovskite ($CsPbI_3$) [3]. The World Economic Forum has included PVK-based solar cells (PSCs) among the top ten emerging technologies of the past year (2016), for their ease of

preparation in comparison to silicon-based devices and their significant photovoltaic performance [4].

These materials, when solution processed, are able to form polycrystalline films with high light absorption capabilities across the solar emission spectrum, long carrier diffusion lengths, small exciton binding energies and small charge recombination rates [2, 5-7]. The successful collection of an electric current following light harvesting is realized sandwiching PVKs within a specific architecture, in which electron and hole-transporting layers (ETL and HTL, respectively) are placed on opposite sides of the photoactive layer, allowing the optimal extraction of opposite charges (electrons and holes respectively) into the external circuit. A large plethora of materials has been studied for the roles of both ETL and HTL. Among them, semiconducting carbon nanomaterials (CNMs) have attracted a significant attention [8]. Fullerenes, either in their pristine form as C_{60} or C_{70} or as chemically modified ones, such as the well-known soluble derivative 6,6-phenyl-C61-butyric acid methyl ester (PCBM), are among the most employed CNMs in PSCs. Their key role, as electron acceptors, has been consolidated in the past by the application they have found in organic photovoltaics (OPV) [9-11]. However, the trend of growth in scientific publications on fullerenes used in OPV (Fig. 1) shows a progressive increase from 1995 (first paper) to the end of 2014 (more than 300 paper), although with a slight decrease in the last two years, (280 papers in 2016).

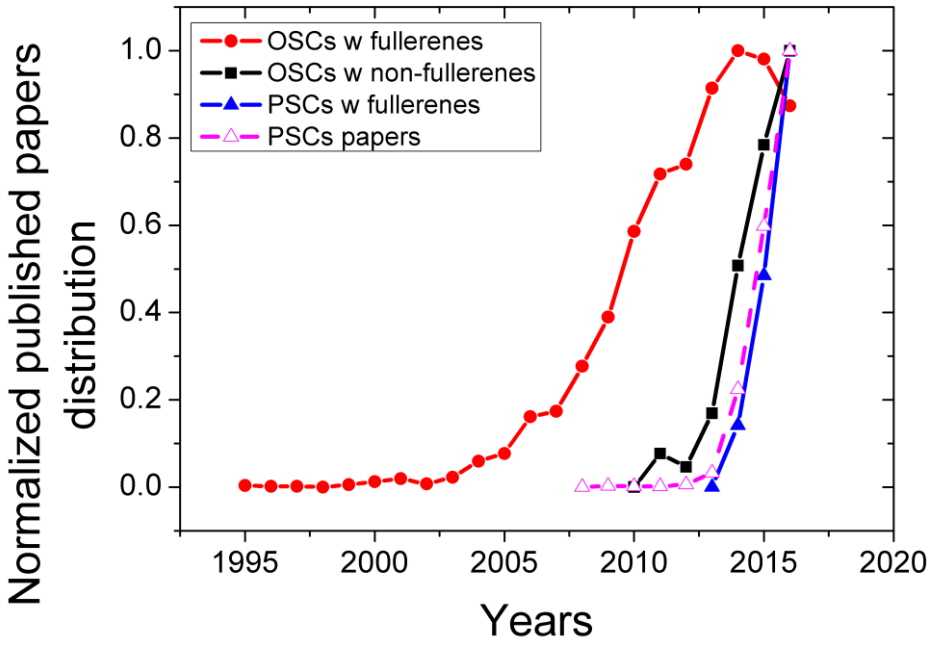

Fig. 1. Summary of published papers (until the end of 2016) taken from Scopus concerning the use of fullerenes in different PV fields. The keywords for the different searches were "organic solar cell* fullerene*" for fullerene acceptors based organic solar cells (OSCs) (red line), "non-fullerene* organic solar cell*" for non-fullerene acceptors based OSCs (black line) and "perovskite solar cell* fullerene*" for PSCs containing fullerenes (blue line). Dashed line with opened triangles represents the trend of published paper on PSCs.

This is most likely due to the nascent interest for non-fullerene acceptors [12-15] started in 2010 (see Fig. 1, from the first paper published in 2010 to the 50 published in 2016). This type of acceptors, such as naphthalene or perylene diimide derivatives, is apparently stealing the ground to fullerenes in OPV applications. They were introduced initially with the aim of producing acceptor materials with LUMO energies higher than those of most fullerenes and thus closer to the majority of donors' LUMOs, being this aspect a possible origin of thermalization losses [16], and also with the aim of extending acceptors light-absorption ability, lacking C_{60} derivatives of pronounced absorption features in the visible range [16]. At the same time, the intention was that of finding a way to overcome the high production costs of fullerenes too (even if they have significantly diminished recently along with progresses made in their synthesis). It is worth mentioning that so far fullerenes remain the best performing acceptors in OPV [13], certainly because of their outstanding electron affinity, electron mobility and ability to form very effective nanoscale percolation pathways for electrons within donor polymer phases.

Focusing the attention on scientific reports dealing with fullerenes together with PSCs one finds a rate of growth significantly higher than that observed for fullerenes and OPV (Fig. 1, blue line), showing that an effective new era for fullerenes started within the realm of PVK technologies. The absolute number of reports coupling the two keywords has in fact moved from 2 papers in 2013 to more than 130 papers in 2016. Interestingly, the same trend is observed in the distribution of published papers on PSCs (more than 3000 in the last three years).

The peculiarities of buckyballs, making them more appealing than other CNMs for PSCs, are first found in the alignment of energy levels, with lowest unoccupied molecular orbitals (LUMOs) matching the conduction band of PVKs, and in the high electron mobility [17-20], even if the second aspect is characteristic also of other CNM [21]. Furthermore, fullerene nanometric-sized spherical shapes result to be very important for an efficient interfacing with PVK, allowing to achieve a homogeneous distribution of the CNM on the surface of the light-absorber, thus generating highly selective contacts for electron extraction. This would be a difficult task to tackle with other types of CNMs, such as graphene-based materials (GBMs) or carbon nanotubes (CNTs), because of their extremely heterogeneous constitutional units within a sample, each having different sizes and properties. As a matter of fact, CNTs are assuming a significant relevance in PSCs only as HTLs, either alone or in combination with other materials, because they can efficiently extract holes from photo-excited PVKs and provide a physical protection for these last ones from environmental damages [8, 22], whereas GBMs are evaluated both as HTLs (more specifically reduced graphene oxide) [23, 24] and as ETLs, in combination with TiO_2 [24, 25]. Interest in CNMs use in PSC is also addressed towards the preparation of flexible transparent electrodes [8].

Within such a framework, the effective roles played by fullerene derivatives in PVK-based solar technologies are analyzed, recalling the major milestone works in the field and keeping a critical view on the topic, which will enable to establish perspectives for the field in the nearby future. A brief introduction on the use of fullerenes in photovoltaics before the advent of PVKs will be the subject of the next paragraph, highlighting the ideas and the established knowledge that drove their successful integration in PSCs.

2. Fullerenes in photovoltaics before perovskites

Use of fullerenes as electron acceptors in organic solar cells (OSCs) allowed writing an entire chapter in the history of optoelectronics, as a key milestone in materials science, located at the real intersection between chemistry, physics and engineering [26]. Fullerene-based electron acceptors [17], together with donor polymers or small molecules, in the configuration universally recognized as "bulk heterojunction" (BHJ) [27], have provided a stable platform, following proper material energy level engineering, optimization of film morphologies and electrical contacts, to reach power conversion efficiencies (PCEs) which are now stabilized around the 10% threshold [28, 29]. Up-to-date reviews on the topic can be found here [9, 30]. As pointed out previously, the remarkable electron affinity of these zero-dimensional CNMs, characterized by largely available electron accepting states [31], combined to the efficient transport of negative charges across well-defined nano-domains, have raised them to the role of prototype electron acceptors in OPV applications. Up to now no other organic systems have been found which are able to provide the same outstanding performance in this role, even if a constant attention is devoted to the design and development of possible alternatives [31]. This has prompted researchers to test fullerenes also in other contexts in which the use of electron accepting molecular species might have contributed significantly in improving PCEs. As a matter of fact, this has been the path which have conducted to the first use of fullerenes in PSCs: for this reason, it is important to outline it here, as we attempt to do briefly in this chapter.

At first instance, it is relevant to recall that fullerene derivatives have been used as interlayers in the so-called inverted organic solar cells (OSCs). In this OSC configuration (see Fig. 2a), pristine or functionalized buckyballs are employed in the form of ultra-thin films or self-assembled monolayers (SAMs) on the surface of inorganic semiconductors (TiO_2 or ZnO, having the role of electron transporting and hole blocking layers), to passivate surface oxygen defects which affect electrical transport across the active layer – ETL interface (see Fig. 2a for a sketch of an inverted OSC architecture indicating the position of the fullerene layer) [32-34].

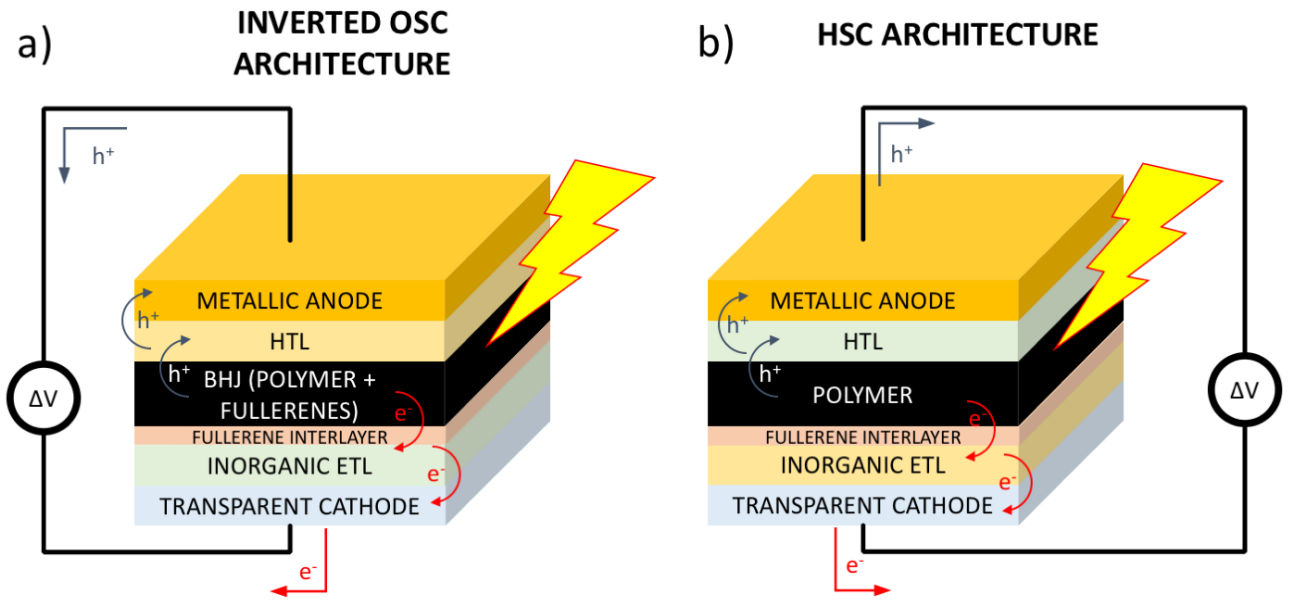

Fig. 2. Schematic representation of a) an inverted OSC architecture and b) organic/inorganic HSC architecture highlighting the position of the fullerene-based interlayers in the cell.

The presence of passivating fullerene species on the metal oxide surface not only allows to improve charge transfer and better tuning of the energy levels, but also drives the formation of an optimized morphology of the next deposited BHJ layer [35]. Strategies to produce fullerene thin films and/or SAMs on top of metal oxides have resorted to proper chemical functionalization of the CNM, with moieties able to establish selective bonds with the ETL, such as carboxylic acids, phosphonic acids or chatecols [32, 36]. In other cases cross-linking, i.e. the formation of covalent bonds networks between neighboring fullerene molecules, was exploited in order to create a chemically stable interlayer [33, 37]. More recently, ethylenediamine-functionalized fullerene nanoparticles were even employed as independent ETLs, allowing to gain higher PCEs compared to the use of a standard ZnO ETL and thus paving the way to metal oxide-free inverted OSCs [38].

On the other hand, fullerene species have attracted the attention as interlayer materials also in organic-inorganic hybrid solar cells (HSCs). These devices are essentially constituted of a semiconducting polymer and a semiconducting metal oxide, in which electrons are injected into the conduction band of the inorganic acceptor directly from the photo-excited polymer donor (see Fig.2b for HSCs architecture, including the position of the fullerene interlayer within it) [39]. Since this architecture suffers from serious efficiency limitations, for reasons which have not been fully clarified yet,[40] the use of fullerenes as thin layers at the interface to promote a more efficient charge transfer from the donor to the acceptor was proposed by Vaynzof et al. already back in 2010 [41]. Phenyl-C61-butyric acid (PCBA) was employed for its ability to selectively bind to a ZnO film in a SAM approach (C_{60}SAM) and to locally generate a permanent dipole, resulting in a favorable increase in the work function of the substrate.[41] In addition, since the photo-induced

electron transfer from a conjugated polymer like poly(3-hexylthiophene) (P3HT) to fullerene is highly favorable, as largely demonstrated with OPV, electrons in this way are also more keen to access the metal oxide conduction band and thus to generate a photo-current. Another approach, aimed at suppressing the detrimental effect on the overall device efficiency of charged traps located in the bulk of the photoanode, was proposed by Deng and coworkers with the incorporation of C_{60} within the inorganic semiconductor (TiO_2) through a sol-gel approach [42]. The obtained composite showed a significant suppression of charge recombination in TiO_2 bulk, since C_{60} units are able to accept electrons in trap states of titania and to transfer them back into its conduction band.

Interestingly, the first use of C_{60} derivatives in PVK based PV devices was as mediators of photo-excited electrons traveling through a donor-acceptor interface. Abrusci et al. [18], proposed the use of C_{60}SAM-functionalized mesoporous TiO_2 photoanode for a solar cell architecture constituted of PVK and P3HT (see Fig. 3b). In this configuration, the device containing the C_{60}SAM was able to provide a PCE exceeding 6.7%, with an open-circuit voltage (V_{OC}) over 0.8 V, in comparison to a 4% PCE and a V_{OC} of ~ 0.7 V obtained from the device without the C_{60}SAM. From this first successful proof started the steady increase of fullerenes applications in PVK solar technology, as reported above. In the next paragraph, a critical overview of the last three years of activity is reported.

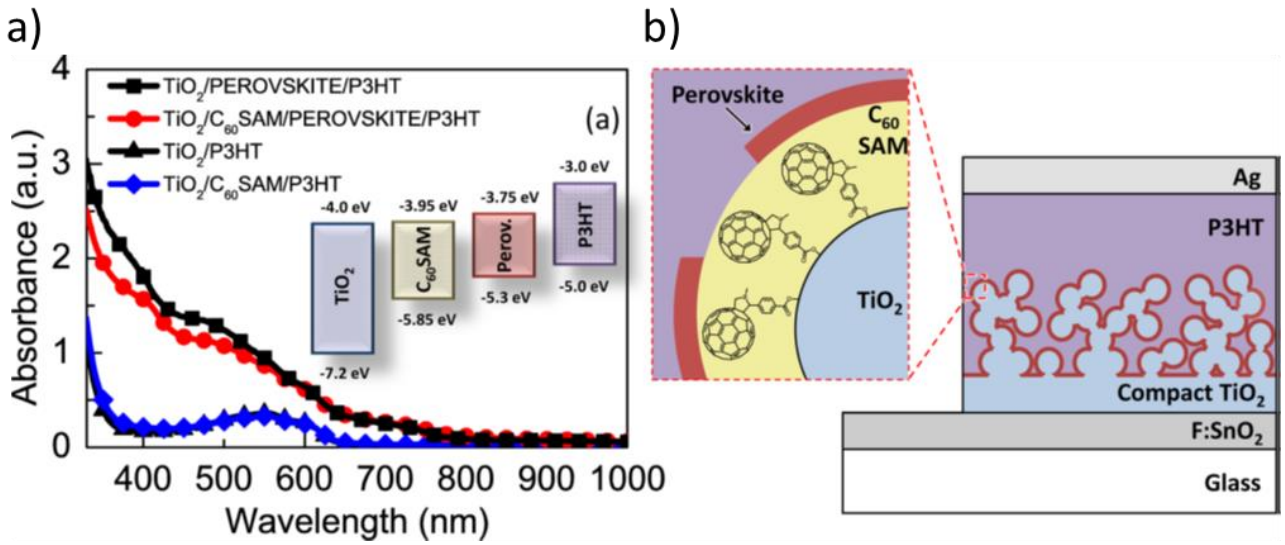

Fig. 3. a) Absorption spectra of P3HT/PVK films on mesoporous TiO_2 with and without a C_{60}SAM interlayer and schematic of materials energy levels vs. vacuum. b) Schematic of Abrusci's device architecture with detail on C_{60}SAM organization on TiO_2. Reprinted from ref [18] with permission from the American Chemical Society.

3. Fullerenes in PSCs

Abrusci's work [18] introduced the use of fullerenes in PSCs. The working architectures of PSCs are sketched in Fig. 4, in which both standard (Fig. 4a) and inverted (Fig. 4b) configurations are

shown. In the standard one, the perovskite film is sandwiched between ETL and HTL with n-i-p-like configuration, whereas in the inverted configuration HTL and ETL are reversed with p-i-n-like configuration. The use of fullerenes as electron mediators and electron transporting materials and the way they are processed, have progressed with the development of PSCs.

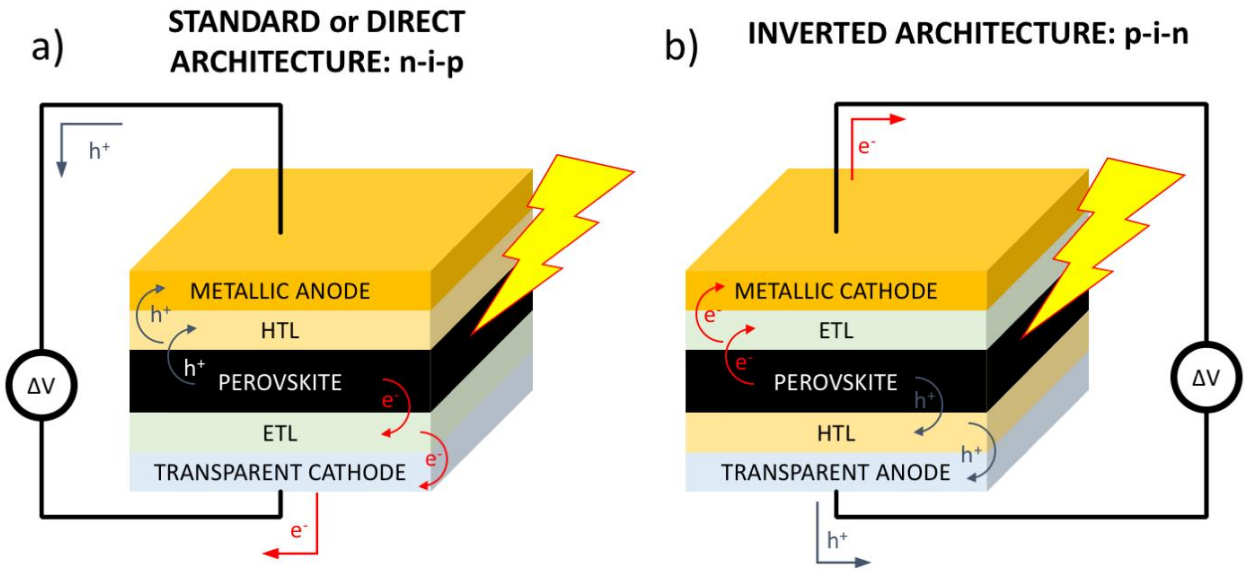

Fig. 4. Schematics showing the two different configurations used for PSCs: a) standard architecture and b) inverted architecture.

3.1 Fullerene mitigates electrical hysteresis in PSCs

In 2014, landmark works came out concerning the integration of fullerene in PSCs [43, 44]. The groundbreaking contribution of Wang et al. [43] showed how fullerenes (in particular a double layer of evaporated C_{60} and spun PCBM or indene C_{60} bis-adduct –ICBA-) can eliminate dark current leakages and how they can act as trap quenchers in inverted PSCs by reducing the trap density of states on the PVK surface (Fig. 5a). Although both forward and backward voltage scans on the devices at low scanning rate gave rise to identical *J-V* curves, the authors did not claim at that time the fact that they produced the first example in the literature of a PSC with substantially no-electrical hysteresis, i.e. a variation of the power output of the cell deriving from the bias history of the PSCs [44]. This architecture allowed to obtain the largest fill factor (FF) (of about 80%, Fig. 5b) for an inverted architecture [43]. Later, Snaith and coworkers highlighted how a C_{60}SAM distributed on a titania-based ETL could significantly reduce the "anomalous electrical hysteresis" [45] in standard architectures. The authors also showed that the extraction properties remarkably increase because of the presence of a higher electron density on the fullerene monolayer (Fig 5c).
Joining the two previously recalled contributions, Huang's group [46] confirmed that fullerenes can passivate a high density of charged traps in PSCs, causing a tremendous boosting of PCE up to

14.9% (due to higher short-circuit current -J_{sc}- and FF). Interestingly, they came to the conclusion that fullerene is able to passivate trap states close to the top surface and along the grain boundaries of PVKs.

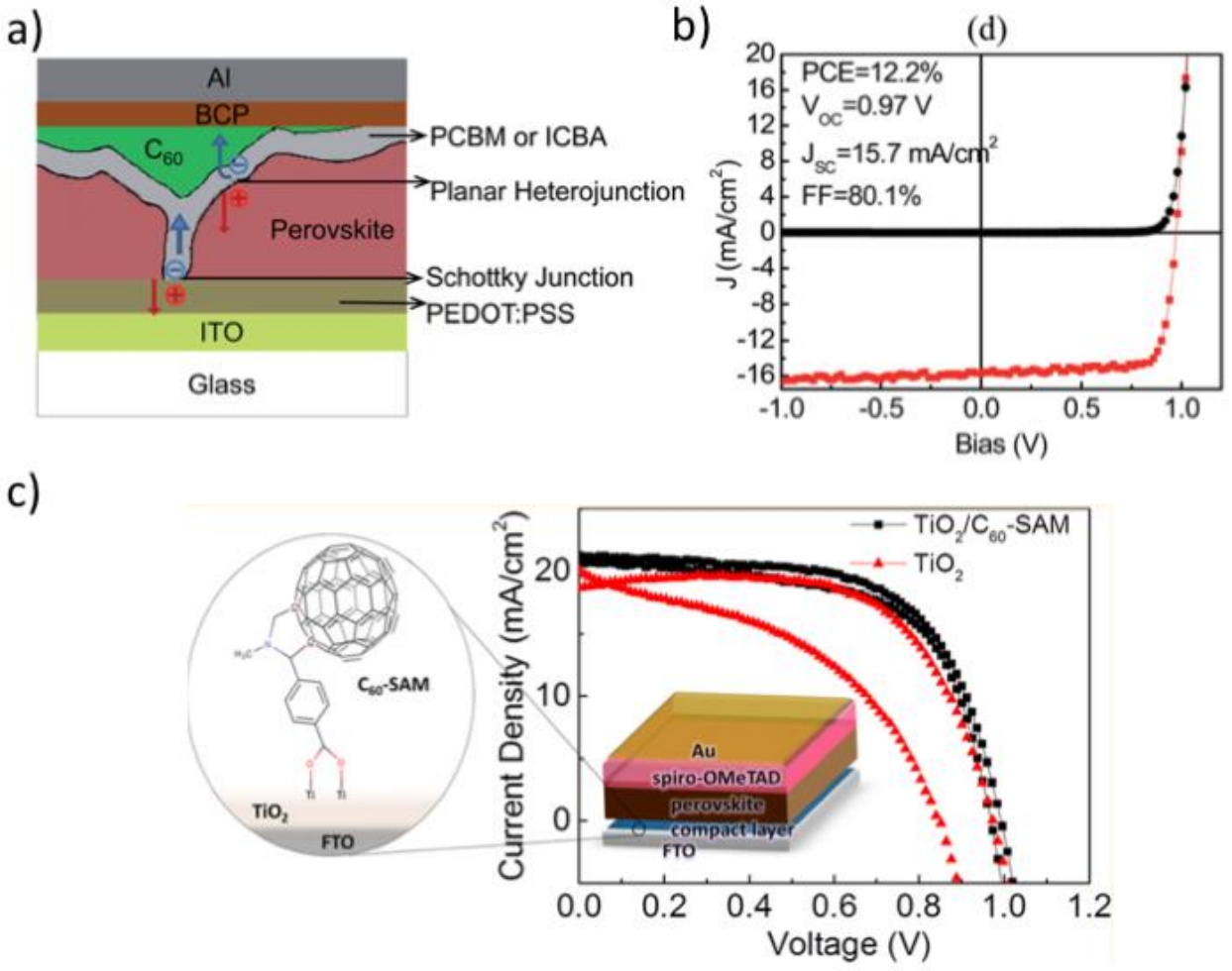

Fig. 5. Landmark works introducing the important role played by fullerene species in PSCs. Reprinted from ref [43] with permission from the Royal Society of Chemistry and ref [44] with permission from the American Chemical Society. a) PCBM or ICBA used together with C_{60} to form a Schottky barrier in an inverted PSC; b) *J-V* curve obtained with this configuration showing the impressive FF of the cell; c) a self-assembled monolayer of fullerenes (C_{60}SAM) dramatically reduces the hysteresis in a direct PSC.

3.2 Processing issues for fullerene integration in PSCs

At the end of 2014 the unsolved problem was still the integration of fullerenes as ETLs in standard architectures because of the fullerene layer dissolution when the PVK is subsequently solution-processed. This is a key limitation in the development of PSCs with high performance, because inverted architectures, in which the fullerene ETL can be easily incorporated as the last step before the evaporation of the top metal electrode, have generally worst PCEs due to an inherently lower Voc. For this reason, general solutions were found by making use of chemically functionalized

fullerenes with different (orthogonal) solvent compatibilities with respect to PVK or in developing cross-linkable fullerene derivatives. This is recognizable as the key step in PSCs development foreseeing the transition from a laboratory limited technology to a real potentially competitive industrial product.

In paragraph 4 of this review, a detailed analysis of the literature reporting on chemical modification or cross-linking of fullerene derivatives for engineering interlayer materials in PSC is reported. Here it is particularly important to recall only the milestone contribution of Chao et al., which were the first to use a cross-linked C_{60} in a standard architecture PSC for modifying a ZnO ETL and through this process achieved 11.9% PCE, suppressing at the same time electrical hysteresis [47].

A notable stabilized PCE (17.6%) was obtained with a different technical approach for the PVK film production, which still avoids any damage of the underlying organic layer, as reported by Tao et al. [48]. In this case indeed, a modified two-steps procedure was used for the PVK film preparation in which the first step is a direct evaporation, on top of spin-coated PCBM, of lead iodide, that is immediately converted into PVK by spin coating on top of it an ethanolic solution of methylammonium iodide (MAI).

3.3 The route towards stable PSCs including fullerene ETLs

Discussions immediately followed to model the fullerene role in the working mechanism of PSC. Liang et al. [49] correlated the electron mobility of fullerenes with device performances, whereas Lo et al. [50] analyzed the thermodynamic role of PCBM and C_{60}. Theoretical calculations revealed that ions can physically move within the perovskite layer causing an irreversible doping, [51] which was confirmed also experimentally [52, 53]. Xu et al. [54] developed a phenomenological model which suggests why fullerenes can solve the problem of hysteresis. They demonstrated, by means of DFT calculations, that the formation of PCBM-halide radical is thermodynamically favored and causes the suppression of trap states. Following this *in situ* passivation, the complete elimination of the electrical hysteresis is expected. In agreement with such picture, some of us have recently shown that perovskite nanocrystals produced by laser ablation in benzene-rich solvents, and thus passivated by carbonaceous material, present virtually no ion migration when displaced in thin films [53]. Moreover, Tao et al. also demonstrated through transient absorption spectroscopy that an efficient charge transfer takes place at the PCBM/PVK interface, significantly improved with respect to the neat TiO_2/PVK interface [48].

One of the major goals to be set for the next future is the possibility to exploit fullerene derivatives to enhance PSC stability. One first step towards the realization of this perspective is the recently demonstrated improved photo-stability to UV light irradiation shown by PSCs containing fullerene

ETLs with respect to those containing c-TiO_2 ETLs [55, 56], characteristic which allows to increase the overall quality of the solar cell [57]. At present, it is completely unknown whether UV-light induced dimerization or polymerization of fullerenes occurs and whether this mechanism might contribute positively or negatively to the final PSC stability. For sure, only in the standard architectures – in which the cell is irradiated from the transparent bottom electrode – this issue would be relevant, since in the inverted architecture the PVK layer itself acts as a UV barrier for the C_{60} layer. There are a few literature reports concerning the possible dimerization/polymerization of fullerenes in BHJ OSCs after light soaking under standard testing conditions [58, 59], which, by increasing the overall extent of fullerene crystalline domains, cause a significant diminishment of the capability to extract charges of these molecular acceptors [60]. With respect to this, the interesting work of Chiang et al. [61] presenting a BHJ PSC with PCBM exhibiting an outstanding FF (more than 80%) leaves open a question mark about whether a continuous illumination might affect the overall stability of the cell in a BHJ PSC configuration as it does in a BHJ OSCs.

However, considering the lower electron mobility of fullerenes species at the solid state with respect to PVKs BHJ PVK/fullerene active layers, one

However, considering the lower electron mobility of fullerenes species at the solid state with respect to PVKs (i.e. 10^{-4}– 10^{-3} cm^2 V^{-1} s^{-1} vs 6–200 cm^2 V^{-1} s^{-1} [62]), it is unlikely that BHJ PVK/fullerene active layers work in the same way as BHJ OSC active layers. Therefore, considering the too large size of the fullerene cage to be hosted within the PVK lattice, one is more prompt to think that the role of fullerenes in BHJ PSCs is limited to that of charge passivating agents for PVK surface defects [63], although there are evidences of the possibility to optimize electron transport in fullerenes at the solid state through proper crystal engineering [64, 65]. On the other hand, it is fair to remind that interface engineering at the nanoscale has been demonstrated to significantly improve the overall quality of the figures of merit for BHJ PSCs [66]. Therefore, considering fullerene as a pure charge passivating agent might be reductive when trying to explain the overall optoelectronic phenomena taking place in BHJ PSCs and further studies are required, as underlined in a recent perspective article also coming from the group of Huang [67], where the role of fullerenes as quenchers for ion migration at PVK grain boundaries is deeply analyzed.

Surface engineering proved to have great importance in the final stability of PSCs [68-72]. Kim et al. showed [73] by means of impedance spectroscopy that the main factor generating hysteresis in a PSC is the excess of charge accumulation at the surface of the commonly used titania-based ETL and that, by replacing the inorganic ETL with PCBM, the hysteresis can be strongly reduced. This work opened the way for a great simplification of cell architectures, since it showed that fullerenes can be directly used as ETLs: a few papers came out demonstrating the feasibility of this approach

[74-79]. Thanks to these works, the standard architecture was also applied to flexible substrates [79] in which C_{60} was used as the unique ETL without the need for an underlying titania layer, this last one requiring high temperature sintering, a process which is not suitable to be applied on flexible substrates. Finally, Wojciechowski et al. reported [80] up to 15% PCE without employing any titania, but simply a thin layer of two types of chemically-modified C_{60} able to cross-link after being spun on the underlying optically transparent electrode (OTE), through thermal/chemical processes and thus forming highly resistant ETLs, not damaged by the subsequent PVK deposition step. Following a similar approach, even a single SAM of silanized-C_{60} was recently deposited on top of the OTE obtaining stabilized PCEs and good quality PVK films [57].

Chiang et al. [61] recently showed the importance of including fullerenes in close contact with PVKs using a BHJ PSCs in which 0.1 wt% PCBM was added inside the PbI_2 layer, then converted into PVK through a solution-based process. Measurements of the charge carrier diffusion length in the perovskite layer showed a substantial increase of this parameter. This methodology allowed to reach the complete elimination of electrical hysteresis, as well as the actual world record in an inverted PSC of 82% FF with a PCE of 16% (see Fig. 6).

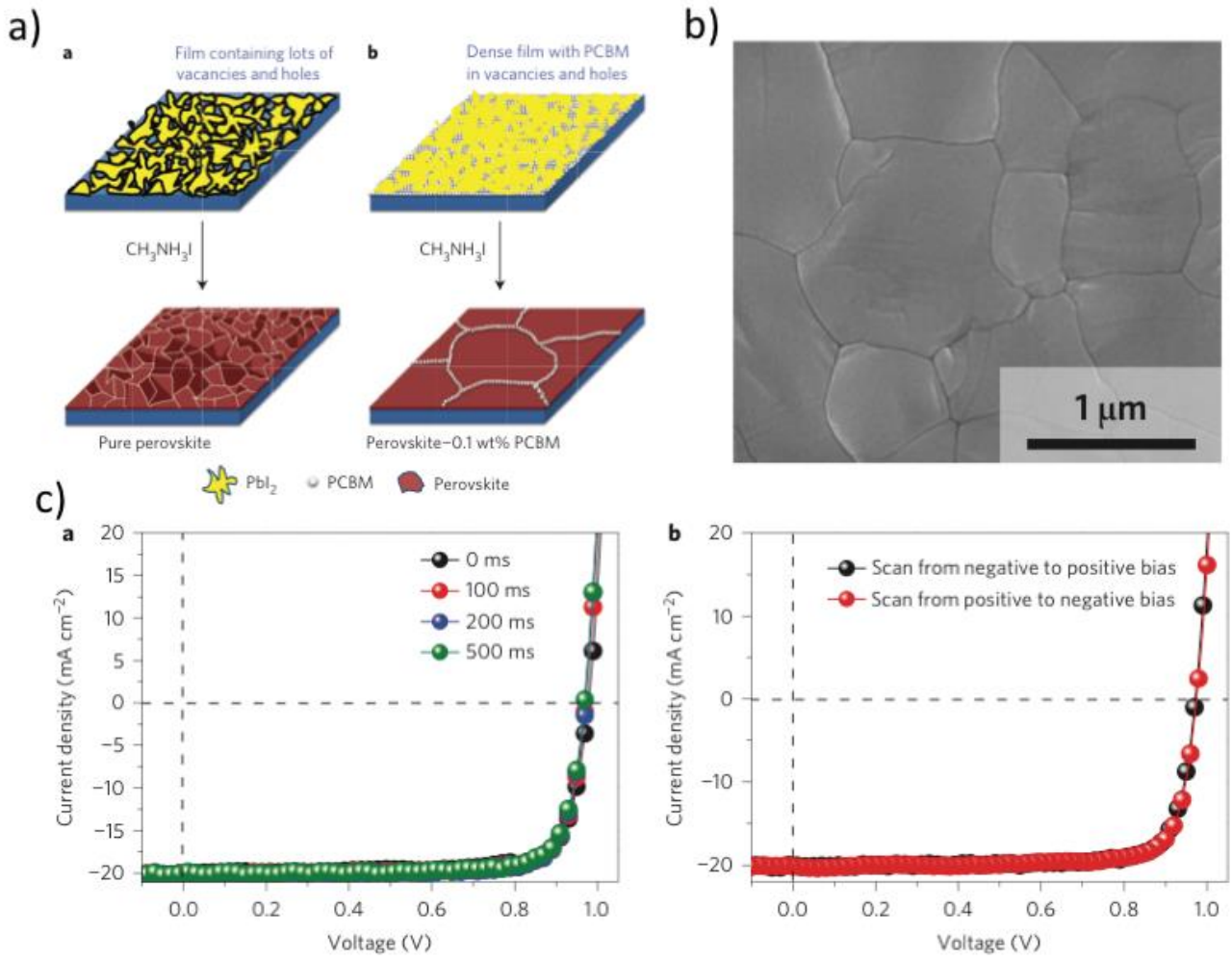

Fig. 6. The highest fill factor achieved in a PSC employing a PVK composite with PCBM, reprinted from ref. [61] with permission from Nature Publishing Group. a) Schematic for the preparation of the composite; b) HR SEM image of micrometric perovskite grains; c) *J-V* characteristics showing complete elimination of hysteresis independently from biasing treatment of the device.

In the next chapter, the existing works addressing further problems, such as those related to PSC stability to environmental and illumination degradation, through the use of particular fullerene derivatives will be presented in detail.

4. Functionalized fullerenes in PSCs

Pristine fullerenes possess intrinsic properties which make them major candidates as part of ETLs in PSCs and they appear to be even suitable for solution processing or thermal evaporation, as thoroughly outlined in the previous sections of this review article. However, the role of a covalent chemical functionalization with different types of organic moieties has been largely recognized as a valuable tool for improving performances of these materials in different contexts and for different applications [81-94]. Besides making fullerenes more soluble in organic solvents or even in water, depending on the type and quantity of functional groups bound to the surface, a particular

decoration can provide many further physical properties, which might be useful to conduct a specific function. For this reason, in this chapter we will give relevance to the most significant examples reported up to now in the literature in which fullerene functionalization with organic groups has been employed to target specific improvement in PVK based devices (excluding the case of PCBM, which is today a sort of benchmark in last generation PV).

The PV properties of PSCs employing chemically modified fullerene species as the ETL are summarized in Table 1.

Table 1. Photovoltaic properties of chemically modified fullerene ETLs

ETL	Name	Cell Architecture[a]	V_{oc} [V]	J_{sc} [mA cm^{-2}]	FF [%]	PCE [%]	PVK	Ref.
1	DMAPA-C_{60}	I	0.97	17.9	77	13.4	$MAPbI_3$	[95]
2	DMDB	D (w TiO_2)	1.13	18.4	71	14.9	$MAPbI_3$	[96]
3	$C_{60}(OH)_{24\text{-}26}$	D (w TiO_2)	0.95	20.9	71.5	14.3	$MAPbI_3$	[97]
4	PCBM+ C_{60}-ETA	D (w TiO_2)	1.05	22.9	66.5	16.3	$MAPbI_3$	[98]
5	c-PCBSD	D (w TiO_2)	1.12	21.1	79	18.7	$MAPbI_3$	[99]
6	$MPMIC_{60}$	D (w TiO_2)	1.08	20.2	64	13.8	$MAPbI_3$	[100]
6	$MPMIC_{60}$	I	0.81	19	78	12.3	$MAPbI_3$	[100]
7	c-PCBCB	D (w/o TiO_2)	1.11	22.4	73	17.9	$MAPbI_3$	[80]
8	Sol-gel C_{60}	D (w/o TiO_2)	1.07	23	73	17.9	$MAPbI_3$	[80]
9	Sil-C_{60} SAM	D (w/o TiO_2)	1.04	19.4	74	15.2	$Cs_{0.175}FA_{0.825}PbI_3$	[57]
10	PTEG-1	I	0.94	20.6	81	15.7	$MAPbI_3$	[101]
11	CLCS	I	1.06	22.7	80	19.3	$MAPbI_3$	[102]
12	D-C_{60}	I	0.96	21.9	79	16.6	$MAPbI_3$	[103]
13	α-bis-PCBM	D (w TiO_2)	1.13	23.9	74	20.8	$FA_{0.81}PbI_{20.85}(MABr)_{0.15}(PbBr_2)_{0.15}$	[104]
14	IS-1	D (w/o TiO_2)[b]	1.03	16.7	69	11.8	$MAPbI_3$	[105]
15	IS-2	D (w/o TiO_2)[b]	1.06	16.1	74	12.7	$MAPbI_3$	[105]
16	PI-2	D (w/o TiO_2)[b]	1.02	16.5	69	11.7	$MAPbI_3$	[105]
17	DPM-6	D (w/o TiO_2)[b]	1.04	16.1	69	11.6	$MAPbI_3$	[105]
18	C_{70}	D (w/o TiO_2)	0.96	14.3	61	8.4	$MAPbI_3$	[106]

[a] D = direct architecture. I = inverted architecture. [b] ETL-free PSCs based on PVK/fullerene blends as active layers.

A particular functionalization of the fullerene backbone can address the resulting derivative towards an increased polarity, as well as allowing the formation of selective interactions with the PVK surface. For example, the role of a dimethylaminopropylamine-C_{60} multi-adduct (DMAPA-C_{60}, **1**) in lowering the work function of metals such as Ag, Cu or Au, previously explored by employing it as a cathode buffer layer in inverted OSC [107], was further confirmed by the study of Azimi and coworkers [95], regarding its use in PSCs. The authors exploited the full compatibility of this material for ambient condition solution processing by means of alcoholic solvents to produce a thin layer of DMAPA-C_{60} as the last step in inverted PSC fabrication, before Ag metal electrode evaporation. PCBM was employed as the ETL (see Fig. 7a for the complete device architecture). The poly(dimethylamino)-derivatized fullerene layer proved to be able to generate an interfacial dipole large enough to suppress the energy barrier between the Ag and PCBM layers (Fig. 7b). Furthermore, the insertion of such a layer reduced significantly the roughness of the surface and

provided a better coverage of the PVK film, thus improving shunt resistance. In this way, an enhanced performance was found for the PSC containing the DMAPA-C_{60} interfacial modifier, with a PCE reaching 13.4% and a significantly better FF in comparison to the device lacking the interlayer (the FF value increased from 61% to 77%).

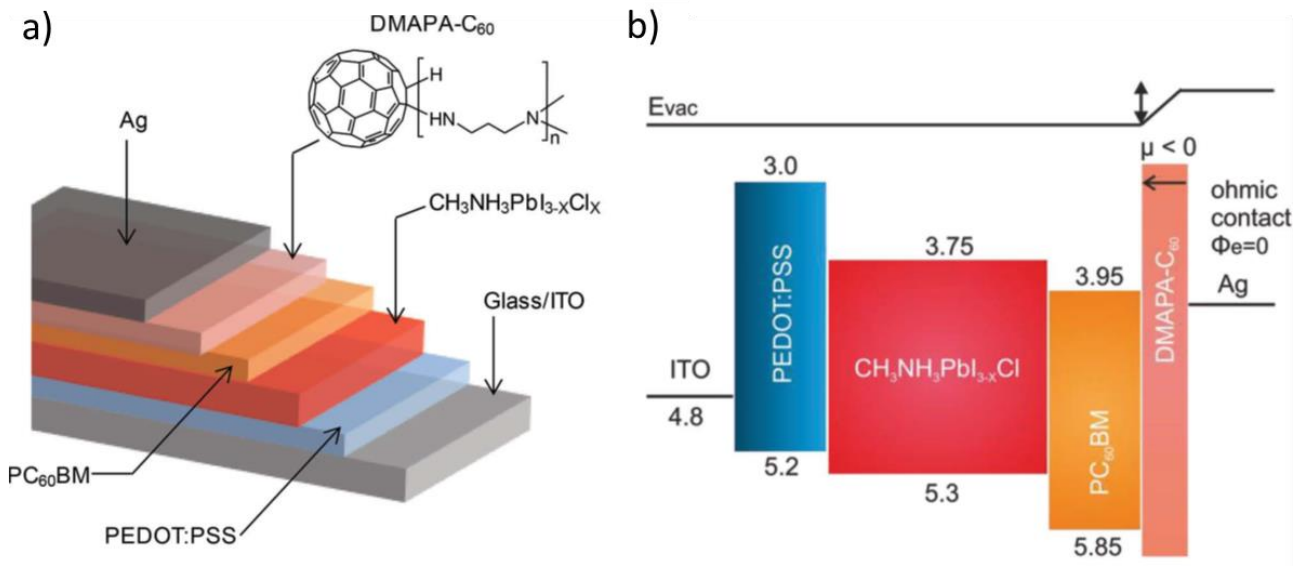

Fig. 7. a) Schematic device architecture of Azimi's inverted PSC with DMAPA-C_{60} interlayer modification. b) Energy level diagram for the device. Reprinted from ref [95] with permission from Wiley-VCH.

4.1 Functionalized fullerenes to overcome processing and stability issues in PSCs

Molecular engineering provides other significant tools to make fullerene layers more stable to the deposition of further layers on top of them, avoiding alteration of their morphology due to not perfectly orthogonal solvents. Different strategies have been envisaged, depending on the particular PSC architecture targeted.

In one case, a thermo-cleavable fullerene derivative, able to establish a covalent bond with the surface of c-TiO_2 after annealing at 170 °C, was employed as passivating agent for reducing charge recombination and hysteresis in a standard architecture PSC [96]. The derivative, namely di-*tert*-butyl methano[60]fullerene-61,61-dicarboxylate (DBMD, **2**), features *tert*-butyl moieties as protecting groups for two carboxylic acids, which ensure good solubility of the compound in organic solvents, enabling efficient solution-processing and obtainment of homogeneous films on top of the titania surface. When film of DBMD are heated at 170 °C, these groups are easily eliminated as 2-methylpropene (a gas), leaving behind the free carboxylic acids that bind tightly to TiO_2. In this way, a stable and homogeneous fullerene coverage of the TiO_2 surface is achieved, making it more hydrophobic and thus inducing the formation of high quality PVK films on top of it. The performance of the resulting devices, in terms of overall efficiencies and elimination of the hysteretic behavior observed when scanning the potential back and forth, is significantly improved

in the presence of the fullerene layer, with almost identical PCEs and FFs in both scanning directions.

Although some authors report that hydrophilic surfaces are preferable for PVK solution-processing, in one case a highly hydrophilic fullerene layer was employed as an interface engineering strategy to enhance wettability of a TiO_2 ETL by means of the DMF solution used for PVK deposition [97]. The specific goal was achieved by using fullerenol, a C_{60} derivative obtained in a one-step reaction with NaOH in the presence of tetrabutylammonium hydroxide and featuring a variable and uncontrolled number of hydroxyl groups on the surface of fullerene comprised between 24 and 26 [$C_{60}(OH)_{24-26}$, **3**], which strongly affect the electronic properties of the molecule. This species is water soluble and forms films of different thicknesses on the surface of c-TiO_2, depending on the concentration of the solution used for spin-coating. The authors tried different thicknesses for the interfacial fullerenol layer and discovered an optimum at 1.5 nm, compared to an optimum for pristine C_{60} of 10 nm. The PSCs performance in the two cases were slightly higher for the fullerenol-based device (PCE = 14.26% against PCE = 13.52% with the C_{60} film), suggesting a better contribution from this last one in reducing interfacial resistance and facilitating charge extraction from PVK to TiO_2 in comparison with bare C_{60}.

The apparent debate, which seems to be arising around wettability requirements for optimal fullerene-based interfacial layers might find an unusual solution in the approach proposed very recently by Chen, Yang and coworkers [98]. In their work, the use of a dual modification of the TiO_2 surface was proposed, employing two different C_{60} derivatives and a two-step surface engineering method. PCBM was used as the first layer on top of TiO_2 with the role of passivating surface traps on the metal oxide, followed by the deposition of a hydrophilic ethanolamine-functionalized fullerene (C_{60}-ETA, **4**) layer improving wettability properties of the PbI_2 PVK precursor solution on the ETL surface. The overall effect of this dual modification of the titania surface led to a dramatic improvement in PSC performance with respect to the use of single modifications (either with PCBM or C_{60}-ETA) and of bare c-TiO_2: PCE reached in fact an average value of 16.31% from values all around 13%, with an almost complete suppression of the hysteretic behavior in the *J-V* response.

Summarizing the different results, a straightforward interpretation about the role of surface polarity at the interface with PVK results not simple: from one side, researchers obtain bigger PVK grains on top of hydrophobic surfaces, but on the other hand overall crystallinity can be lower. In addition, the outcomes can be influenced not only by the polarity of the layers but also by the type of intermolecular interactions established at the interface between PVK and the fullerene layer, which might play a major role in regulating the charge injection process. Therefore, much work has to be

done in this direction to deeply understand the role of surface polarity and chemistry in driving PVK films formation and final PSC operation.

Another approach to fullerene layer stabilization, which is attracting increasing attention, is the use of cross-linkable materials, as was already pioneered in inverted OSC [33], which can be easily deposited in a first step from solution and then cured (either chemically or thermally) to induce the formation of a covalent bonds network among single molecular species, making the layer resistant to further contact with other solvents. For this reason, C_{60} derivatives bearing functional groups suitable as cross-linking units have been developed.

Styryl units have been those mostly employed, with three significant examples from the literature: for two of them the same C_{60} species was employed, namely a [6,6]-phenyl-C_{61}-butyric styryl dendron ester (PCBSD), containing two pendant styrene groups [47] [99], while for the third a mono-styryl fulleropyrrolidine was selected, namely 1-(*p*-phenoxy-(*p*-methylvinylbenzene)indolino[2,3][60]fullerene ($MPMIC_{60}$) (see Fig. 8 for molecular structures) [100].

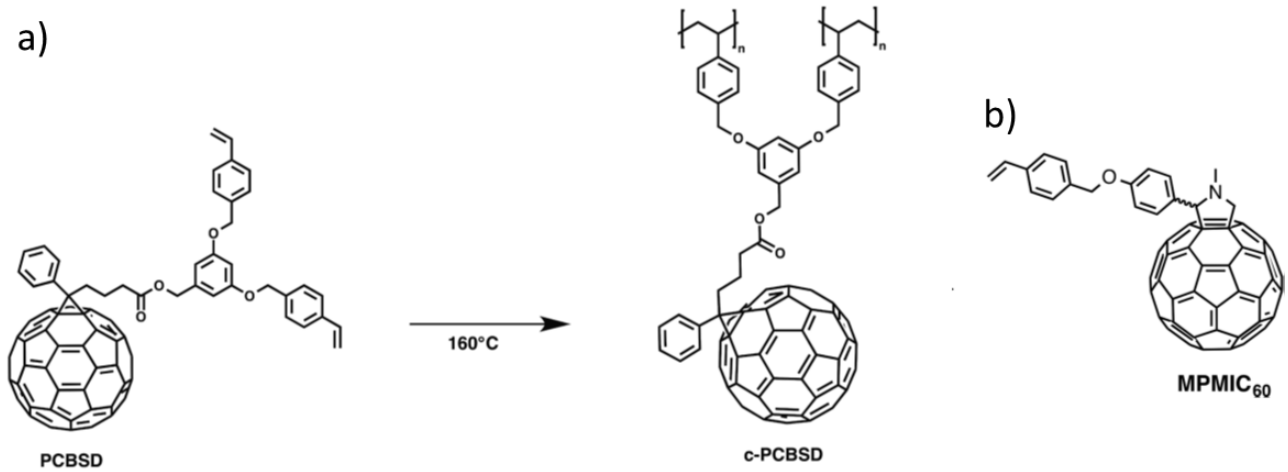

Fig. 8. a) Molecular structure of PCBSD and mechanism of thermal cross-linking, reprinted from ref [99] with permission from Wiley-VCH. b) Molecular structure of $MPMIC_{60}$, reprinted from ref [100] with permission from the American Chemical Society.

Particularly, PCBSD (**5**) has been used as a selective contact for electron extraction in a planar PSC on top of c-TiO_2 [99]. The kinetics of thermal cross-linking (160 °C) was followed by *in-situ* IR spectroscopy, showing that after 45 min the conversion of the carbon atoms in vinyl groups from sp^2 hybridization to sp^3 has reached 35%. This degree of conversion was then demonstrated to be enough for the obtainment of a layer resistant to the subsequent deposition of the PVK precursor dissolved in DMF. Furthermore, electron mobility was also measured, in order to verify whether the cross-linking process had a detrimental effect on such an essential property for ETLs: the cross-linked PCBSD (c-PCBSD) layer tested in a field-effect transistor geometry demonstrated to sustain

in-plane electron transport (ET) over a few micrometers and transversal ET estimated over tens of nanometers. Such a stable thin (10-20 nm) hydrophobic layer proved to be perfectly suitable to induce the formation of large PVK grains (> 1 μm), with average sizes much larger than those obtained by growing the PVK film on top of bare c-TiO_2. The final average PCE for the PSCs containing the c-PCBSD ETL reached 19%, with very good FF (80%) and, particularly, no hysteretic behavior, again confirming the fundamental role of C_{60} species in buffering this phenomenon, which can strongly alter the reliability of standard device testing procedures. In addition, the influence exerted by the c-PCBSD organic layer on the high V_{oc} (more than 1.1 V) was demonstrated. By means of transient photovoltage measurements the authors showed how such a PSC containing TiO_2/c-PCBSD as the electron selective contact has longer charge carrier lifetimes and lower recombination losses than analogous devices based on bare TiO_2 or on TiO_2/PCBM ETLs (Fig. 9).

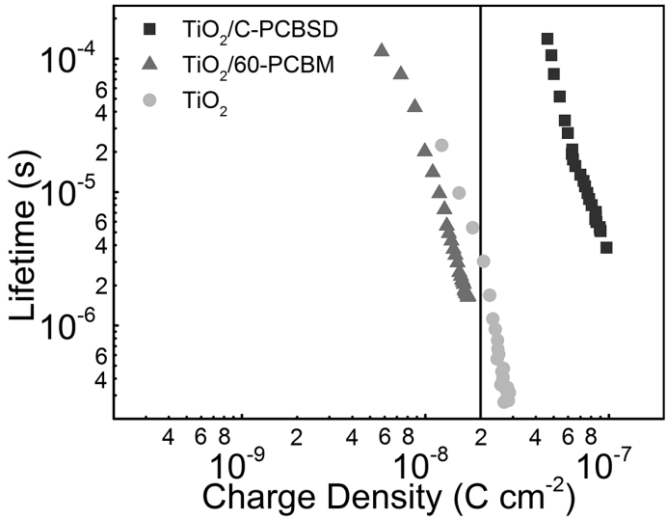

Fig. 9. Recombination lifetime versus charge density deduced from transient photovoltage measurements of PSCs containing TiO_2, TiO_2/PCBM, and TiO_2/C-PCBSD as the electron selective contacts. Reprinted from ref [99] with permission of Wiley-VCH.

The mono-styryl derivatized fulleropyrrolidine $MPMIC_{60}$ (**6**), proposed by Dauskardt, McGehee and coworkers, was developed with the aim of producing a novel cross-linkable C_{60} derivative capable of being thermally cured without the need of any initiator and whose resulting films after the required heat-treatment would gain stability to solvents and, moreover, improved mechanical properties. This last aspect was judged crucial to diminish chances of stress-induced failures within the PVK film, which in turn can cause sub-optimal charge transport and facilitate infiltration of water or other chemicals noxious for the PVK itself. The new ETL demonstrated its beneficial effect also in contributing to good PSC performance, with PCEs higher or comparable to those obtained by employing C_{60} or PCBM as the ETL in both the device architectures tested, but with

enhanced mechanical resistance.

A derivative of PCBM containing a benzocyclobutene functionality, phenyl-C61-butyric acid benzocyclobutene ester (PCBCB, **7**, Fig. 10a), was chosen by Wojciechowski et al. as the candidate ETL in a n-i-p like PSC to be deposited directly on the transparent conductive oxide (TCO) omitting the c-TiO_2 layer, for its ability to thermally cross-link when annealed at 200 °C [80]. The cross-linking process in this derivative involves the benzocyclobutene moiety, which undergoes thermal ring-opening of the four-membered cyclobutene ring to generate a 5,6-dimethylenecyclohexa-1,3-diene intermediate, in turn subjected to an irreversible cycloaddition to form a cyclooctadiene ring, reacting finally with an analogous species or with double bonds within C_{60}. In this way, dimers, oligomers and polymers are generated at the same time [108], yielding a highly insoluble material. Fullerene-based ETLs with a low amount of visible aggregates were thus produced, with average film thicknesses of 15 nm. By employing the cross-linked PCBCB (c-PCBCB) as the electron selective contact, the authors build highly simplified PSCs (FTO/c-PCBCB/PVK/spiro-OMeTAD/Au), demonstrating a stabilized PCE, measured close to maximum power point, of 15.2% (Fig. 10b), which is undoubtedly a major goal for a PVK based device lacking the c-TiO_2 ETL. Within the same work [80], the authors reported also, for the first time in PSC applications, the use of a fulleropyrrolidine featuring the triethoxysilane moiety, *N*-[3-(triethoxysilyl)propyl]-2-carbomethoxy-3,4-fulleropyrrolidine, capable of undergoing a sol-gel process when, after spin-coating deposition, it is treated with trifluoracetic acid vapors (the derivative was in fact named sol-gel C_{60}, **8**, Fig. 10a). The process involves hydrolysis of the ethoxysilane groups to generate covalent networks through the formation of Si-O-Si motifs: in this way a cross-linking is induced, after which the fullerene film becomes very stable to potential re-dissolution. This second type of ETL proposed by the authors performs even better than the c-PCBCB above described: stabilized PCE reaches in fact 16.6% for the best cell (Fig. 11b), which is an even more encouraging result. Both cases employing cross-linked fullerene ETLs outperformed the reference employing a bare C_{60} ETL. The lower performance derived when using the reference material was interpreted as the effect of partial solvent-induced dissolution of the ETL during the subsequent processing of PVK from DMF.

The elimination of titania from PSCs would be highly beneficial from the perspective of bringing this technology into the realm of industrial production. Nevertheless anatase TiO_2 being a very selective and efficient ETL, it requires high temperature sintering (around 500 °C) to be produced and have shown to generate electrical instability in PSCs and long-term damages due to UV-degradation [109], as was already pointed out previously. With this aim in mind, we were attracted by the same siloxane-functionalized fulleropyrrolidine derivative used by Wojciechowski and co-

authors, which was originally developed within our laboratories [110]. We actually reasoned that such a derivative, named by us Sil-C_{60}, would have been able to directly bind covalently to the FTO

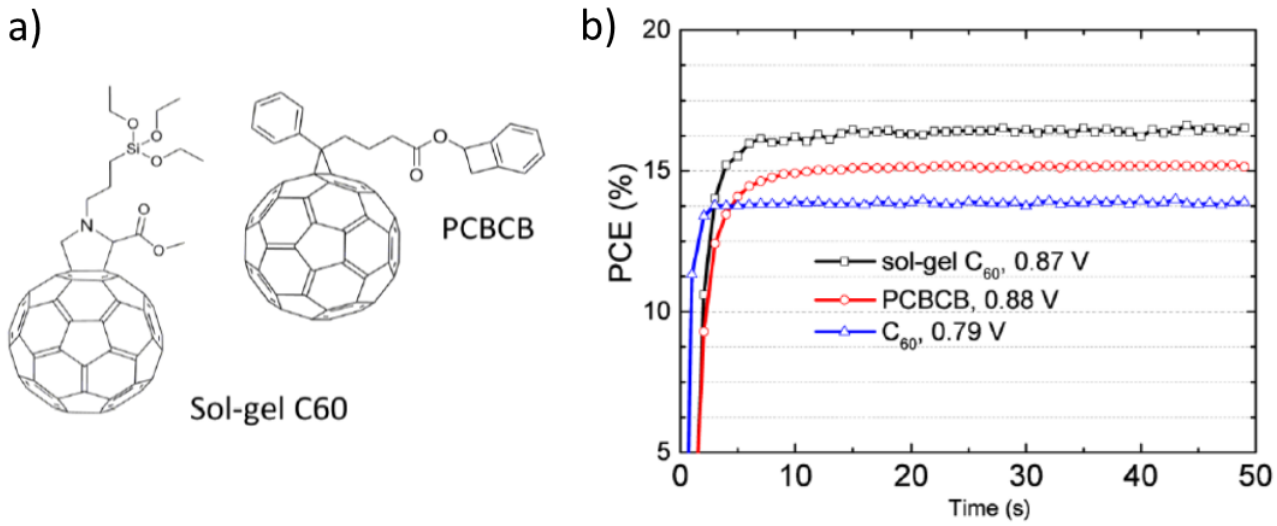

Fig. 10. a) Molecular structures of sol-gel C_{60} and PCBCB. b) Stabilized PCEs for PSCs containing sol-gel C_{60}, PCBCB and bare C_{60} ETLs. Reprinted from ref [80] with permission of the American Chemical Society.

surface, forming a SAM such as those commonly obtained when applying the silanization process to make organic coatings on glasses. The effective formation of a fullerene monolayer, homogeneously distributed on FTO with a high degree of coverage was demonstrated by means of electrochemical impedance spectroscopy sustained by theoretical calculations to estimate the effective thickness of a Sil-C_{60} SAM (**9**, Fig. 11a). Theory and experiment revealed very similar values (1.46 vs 1.4 nm) providing a strong proof for the existence of a monolayer. The electron selective contact constituted of the Sil-C_{60} SAM on FTO was used in n-i-p-like PSC and compared to spin-coated C_{60} on FTO (layer thickness about 20 nm) and to c-TiO_2 on FTO. The two fullerene containing PSCs had substantially diminished hysteretic behavior in sharp contrast to those containing titania. Furthermore, they had quite comparable stabilized PCEs, around the 15% threshold. Anyway, in Sil-C_{60} SAM containing PSC the amount of fullerene material used is significantly lower and furthermore the operation for producing it is much more reproducible. The devices were also tested for stability to UV exposure, confirming the expected results: those containing c-TiO_2 underwent a progressive degradation over 67 h, whereas both the fullerene containing ones did not suffer significantly from the treatment, with the Sil-C_{60} SAM based ones showing the best trend (Fig. 11b).

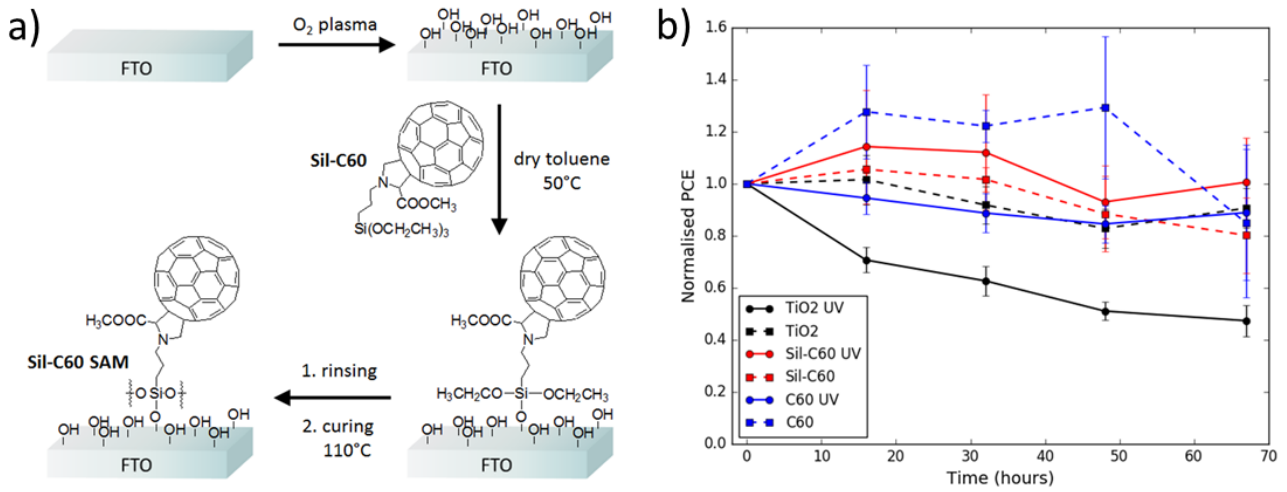

Fig. 11. a) Process for the fabrication of Sil-C_{60} SAM. b) Stability of PSCs based on c-TiO_2, Sil-C_{60} SAM and C_{60} ETLs to UV continuous irradiation over 67 hours. Reprinted from ref [57] with permission of the Royal Society of Chemistry.

Stability concerns are progressively raising everyday more within the scientific community working in the field as major obstacles to surpass before effectively starting an industrial production of PSC modules [111-113]. Attempts to make longer device lifetimes are numerous and reporting on them goes beyond the intention of this review, as well as describing PVK degradation mechanisms. It is instead important to highlight here those cases reported in the literature in which fullerene derivatives have been used to tackle stability challenges, leading to prolonged activity of PSCs kept under environmental conditions.

The light-soaking effect in PSCs can affect long-term stability. The origin of this effect is still under debate [55, 114, 115], but recently the interesting work proposed by the groups of Loi and Hummelen [101] unraveled the existence of a correlation between the dielectric constants of neighboring materials. The use of a fulleropyrrolidine functionalized with a glycol monoethylether side chain (PTEG-1, **10**, Fig. 12b) having a dielectric constant significantly bigger than PCBM (from 3.9 to 5.9), was in fact envisaged to better match the dielectric constant of PVK, which is reported to have values higher than 6.5. By following this idea, it was demonstrated that the light-soaking effect can be significantly reduced. In fact, together with providing a significantly improved PCE when used as ETL in comparison to PCBM (15.7% vs 11.7%), PTEG-1 also contributed to make light soaking a negligible phenomenon. In fact, PCE resulted almost unvaried before and after 1.5 h exposure to light irradiation under the solar simulator for the case of the PTEG-1 containing device (Fig. 12d), considerably different from what happened for the PCBM containing one (Fig. 12c). The authors further investigated the physical reasons behind the different PV behaviors given by the two fullerenes and effectively proved the synergistic effect of higher dielectric constant and electron donating properties in contributing to the enhanced performance obtained with PTEG-1 in comparison to PCBM. The oxygen-rich moieties in the PTEG-1 side

chain and the nitrogen moiety in the pyrrolidine ring may actively contribute at passivating those trap states on the surface of PVK which are generated by halide vacancies, acting as Lewis bases. In this way, trap-assisted charge recombination can be considerably reduced, suggesting the possibility of future improvements through a further fine-tuning of the fullerene chemical functionalization.

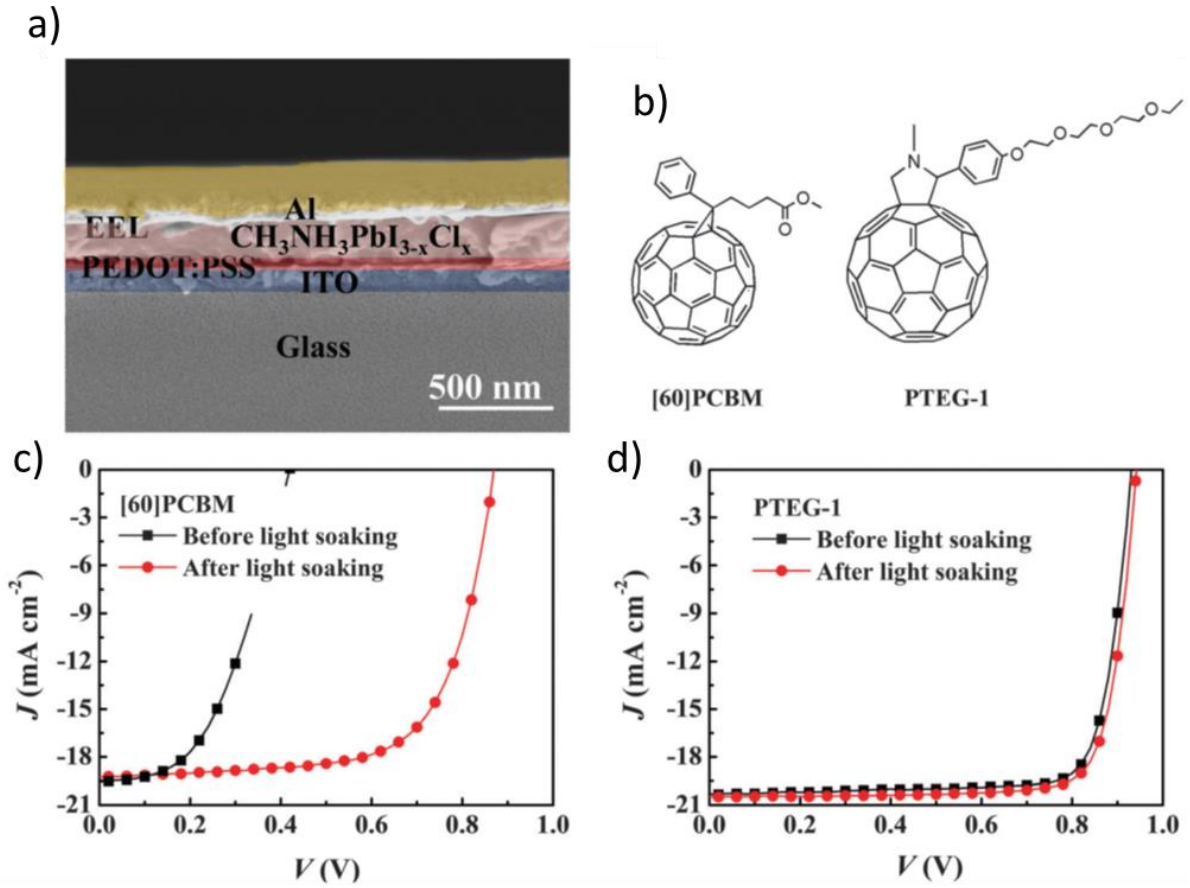

Fig. 12. a) SEM image of Loi's and Hummelen's inverted PSC. b) Molecular structures of PCBM and PTEG-1. *J-V* characteristics under illumination for devices containing PCBM c) and PTEG-1 interlayers d). Reprinted from ref [101] with permission of Royal Society of Chemistry.

A case in which a cross-linking strategy was exploited within an inverted architecture to protect the underneath PVK layer from moisture deserve a particular attention [102]. The chemical strategy selected by the group of Huang, made use once again of silane molecules, bearing highly hydrophobic, fluorinated tails. These molecules can self-assemble through hydrogen bonding interactions on a pre-assembled C_{60}-SAM (made of the same C_{60} derivative functionalized with benzoic acid used by Abrusci et al. in ref. [18]) and cross-link with neighboring ones through formation of siloxane bridges (see Fig. 13a for a sketch of the layers). The PSC containing the cross-linked C_{60}-SAM (CLCS, **11**) demonstrated a significantly higher stability under environmental conditions with respect to a reference PSC containing bare PCBM as the ETL (see Fig. 13b-d), with an impressive initial PCE of 19.5% dropped to only its 90% after 30 days of

continuous illumination in highly humid air, while the reference lost the majority of the initial PCE within 36 h.

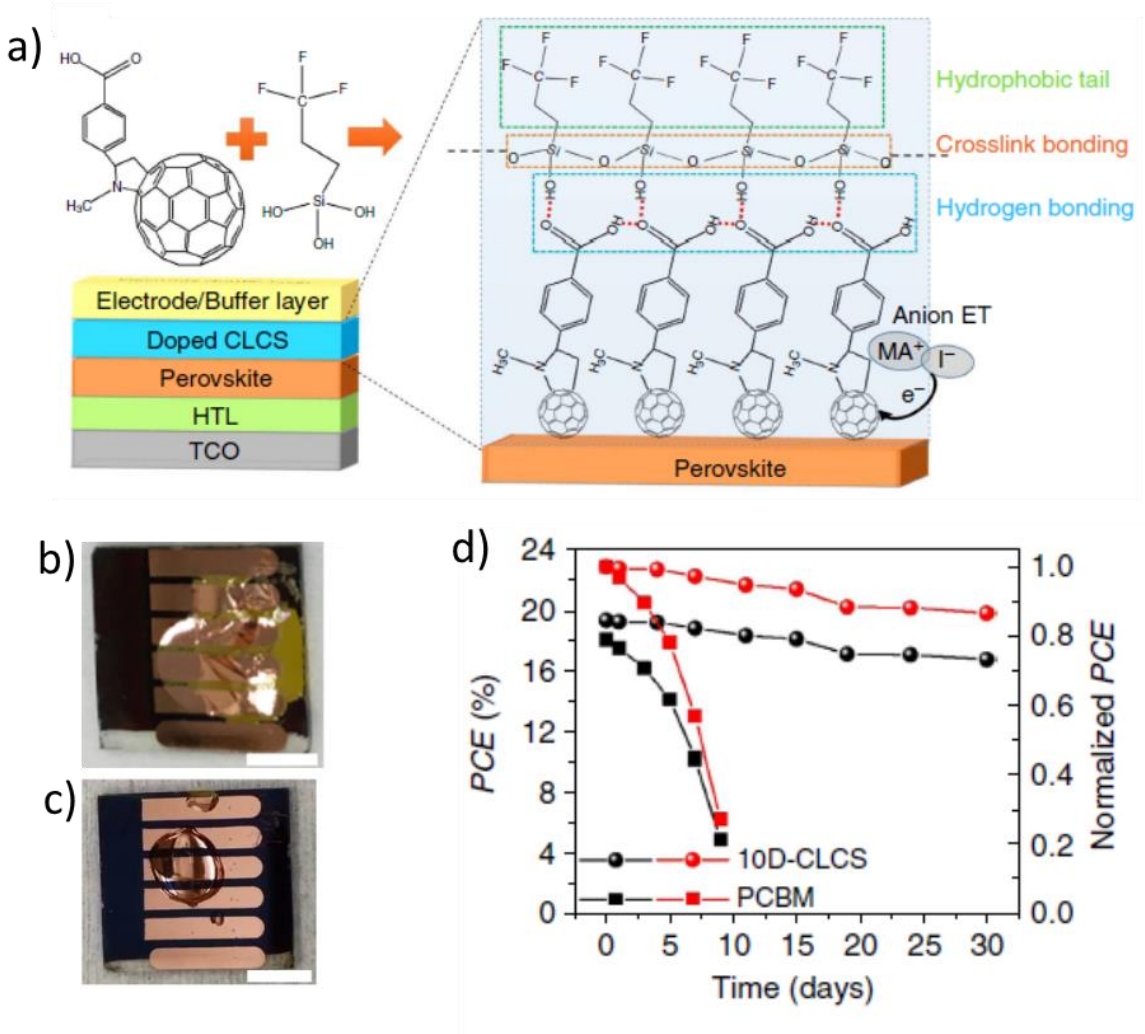

Fig.13. a) Sketch of the PSC proposed by Huang and coworkers containing the cross-linked silane layer on top of the C_{60}-SAM. Images of PSCs containing a PCBM ETL b) and the cross-linked C_{60}-SAM (CLCS) ETL after exposure to water droplets for 4 min. d) Trends in PCEs over 30 days for PSC containing PCBM and CLCS ETLs (black curves indicated absolute performances and red curves normalized ones). Reprinted from ref [102] with permission of Nature Publishing Group.

Following the same idea of creating a hydrophobic fullerene layer on top of PVK in an inverted PSC to boost device stability, Echegoyen and coworkers developed a dimer of PCBM (D-C_{60}, **12**, Fig. 14a), having very similar energy levels to PCBM (Fig. 14b) [103]. The new dimeric species proved effectively to be able to passivate surface traps of PVK and to extract electrons from it as efficiently as PCBM. The PSC containing D-C_{60} as the ETL had better performance than the PCBM based one, reaching a stabilized PCE of 16.5% vs a 14.5% obtained with the reference ETL. An endurance test performed over 350 h also demonstrated the effect of the fullerene dimer ETL on device stability: an efficiency drop to more than 75% of its initial value was detected for the PSC

containing D-C_{60} after this time, while for the PSC with PCBM only the 25% was retained (Fig. 14c).

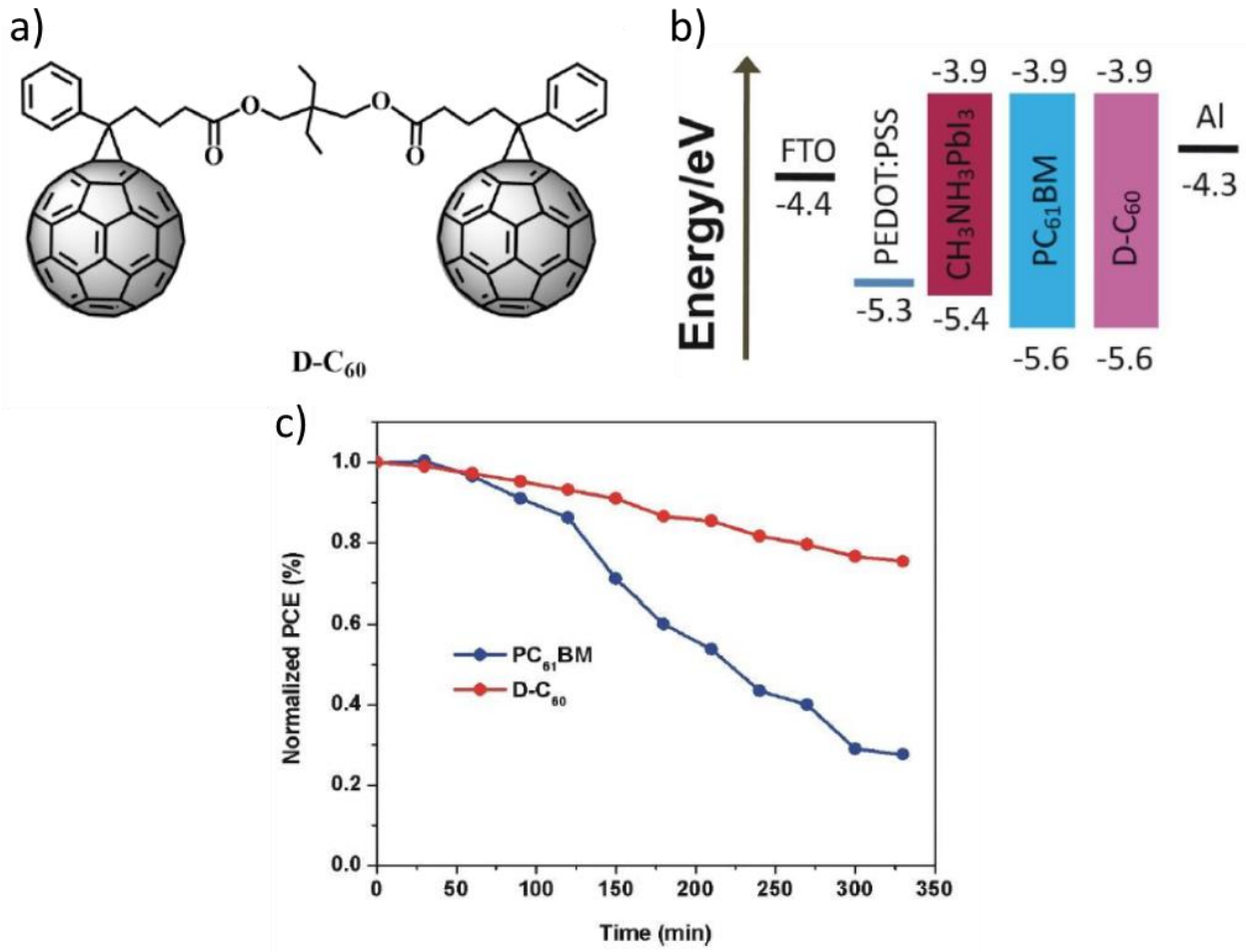

Fig. 14. a) Molecular structure of PCBM dimer D-C_{60}. b) Energy level diagram of inverted PSC containing either PCBM or D-C_{60} as the ETL. c) Efficiency trend of PSCs containing D-C_{60} and PCBM ETLs stored in air as a function of time. Reprinted from ref [103] with permission of the Royal Society of Chemistry.

Graetzel and coworkers reported on the use of one single pure isomer of bis-PCBM (a C_{60} derivative featuring two butyric acid methyl ester moieties), the most abundant one, named α-bis-PCBM (**13**), as a templating agent to enhance the electronic quality, PV performance and stability under heat and illumination of solution processed PVK films [104]. The compound was employed as an additive within the antisolvent added as the last step of PVK film formation, to template the nucleation and growth of PVK crystals. Both bare PCBM and α-bis-PCBM allowed to obtain larger and higher quality PVK crystals as compared to the control sample, lacking of any additive during the antisolvent step. By employing the α-bis-PCBM additive, both stabilized power output and PCE of the resulting PSC were improved with respect to control devices and PCBM-containing ones (a large set of devices for each case was tested). This derivatives demonstrates in fact a superior ability to lower defects concentration in PVK films, as was inferred by time-resolved photoluminescence

(TRPL) decay measurements. Detailed endurance tests were taken in order to determine the contribution to device stability of the new fullerene derivative in comparison to PCBM and to the reference without any additive, namely in i) an ambient environment with 40% relative humidity without encapsulation, ii) an ambient environment with 40% relative humidity at 65 °C with encapsulation for 44 days and iii) under continuous full-sun illumination in a nitrogen atmosphere at room temperature for 600 h. In all the three cases, the PSCs containing α-bis-PCBM outperformed the other two, demonstrating a much longer resistance to degradation. This further proves the validity of choosing the right fullerene derivative, even if employed at the concentrations used for additives, to drive device performances towards brighter perspectives for effective commercialization.

A detailed study on the effect of a series of novel fullerene derivatives with pronounced electron accepting capabilities on the efficiency and stability of ETL-free PSCs based on PVK/fullerene blends as the active layers was reported very recently by Delgado and coworkers [105]. The novel electron-accepting derivatives, shown in Figure 15a, are two types of isoxazolino[60]fullerene molecules (IS-1 and IS-2, **14** and **15**) and two types of pyrazolino[60]fullerene molecules (PI-1 and PI-2, **17**), both bearing highly electron withdrawing fluorine atoms on the phenyl ring pendant substituents. Their effect on PSCs performance are compared with those of two well-known methano[60]fullerene derivatives, namely DPM-6 (**17**) and PCBM (PI-1 was not tested in blend PSCs due to its lack of solubility in DMF). Figure 15b reports the *J-V* characteristics extracted from the ETL-free, PVK/fullerene blends based devices: significantly higher short circuit current (J_{SC}) values are found in devices containing the new strong electron-accepting fullerene derivatives IS-1, IS-2 and PI-2 and the DPM-6 derivative with respect to reference devices based on PVK/PCBM and PVK/C_{60} blends. This behavior is due to the higher solubility of these molecules in DMF, which allows to prepare blends with PVK containing higher percentage of fullerenes. The type of functionality attached to the buckyball seems also to influence the final device performance, with an apparent relation between electron-accepting properties and V_{OC}, which anyway needs to be further investigated. The stability in time under continuous illumination of the best performing PSCs per type of functionalized fullerene species (namely IS-2, PI-2 and DPM-6) were tested on non-encapsulated devices and compared to that obtained by employing pristine fullerene and to that of a fullerene-free device. The trends in PCEs over 240 min are reported in Figure 15c. No significant differences in photostability are found among PSCs containing fullerenes, whereas for the fullerene-free PSC an immediate drop in PCE is observed, which goes to zero in slightly more than 40 min. Based on these evidences, a role of the fullerene core itself in boosting stability of PSCs based on PVK/fullerene blends is ruled out.

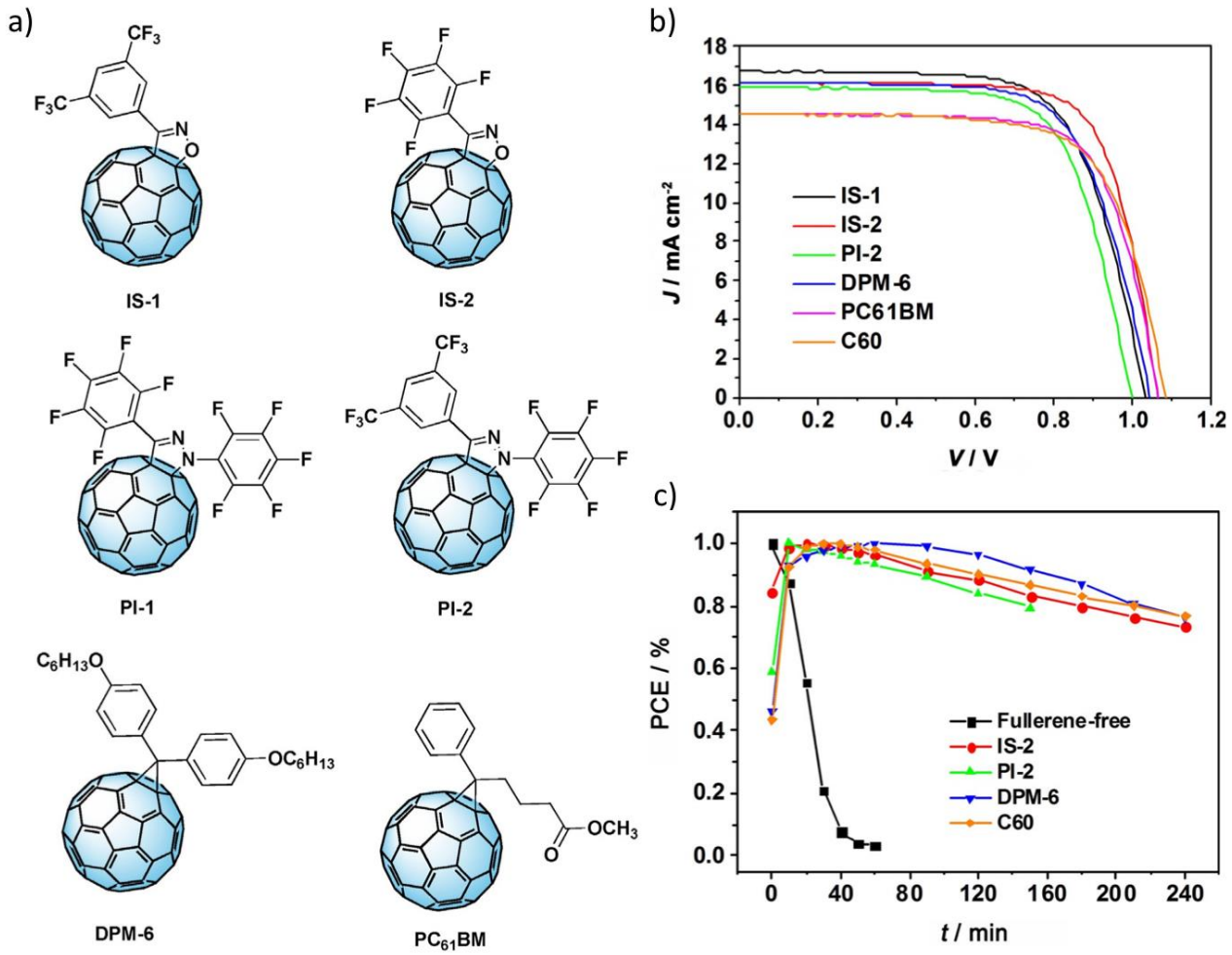

Fig. 15. a) Novel fullerene derivatives prepared by Delgado and coworkers and tested in ETL-free PSCs based on $CH_3NH_3PbI_3$/fullerene blends [105]. b) *J-V* characteristics of the best ETL-free PSCs based on $CH_3NH_3PbI_3$/fullerene blends. c) Evolution of normalized PCE vs time under AM 1.5 simulated sunlight for non-encapsulated solar cells containing the best working fullerene for each type. Reprinted from ref [105] with permission of Wiley-VCH.

4.2 Use of C_{70} in PSCs

As an alternative to C_{60}, the use of [70]fullerene (C_{70}, **18**) as ETL was proposed for the first time by Delgado and coworkers [106], with the intention of exploring the effect of this buckyball, which is known to have similar energy levels to C_{60} as well as to be an electron acceptor, but with significantly lower electron mobility and optical absorption properties spanning over a large region of the visible spectrum. These apparently limiting properties for a PSC ETL were demonstrated to be not so significant in determining the final performance of devices containing C_{70} in substitution to C_{60}: comparable PCEs were obtained by employing the two different fullerenes in n-i-p-like configurations lacking c-TiO_2 and good perspectives were thus opened for the introduction of novel candidates in the plethora of promising CNMs supporting the rise of PVK based technologies, through the exploitation of vacuum-free low-temperature processing and BHJ PVK/fullerene systems, because of the higher solubility in DMF of C_{70} compared to C_{60}. This last aspect was

exploited to lower the amount of dissolution-induced damages on the fullerene based ETL after deposition of the PVK precursor, in the so-called fullerene saturation approach [106]: the saturation of the PVK processing solution with C_{70} before deposition resulted indeed to be an efficient strategy to avoid the dissolution of the C_{70} film based ETL and consequently a universal protocol to improve the performance of PSCs.

The interest in C_{70} is progressively rising: after the first example by the group of Delgado, other works appeared employing this derivative in PSC, as thin layer [77, 116] or in BHJ with PVK crystals [117]. This last work, also authored by Delgado and coworkers, is of particular interest because is the first example of ETL-free PSC containing a PVK/fullerene blend as the active layer (a more recent example has been described at the end of the previous paragraph, also coming from the same research group). The ETL-free direct architecture containing the PVK/C_{70} blend demonstrates a slower charge recombination rate with respect to an analogous one based on the pure PVK active layer and a lower charge transport resistance with respect to a standard architecture with classical c-TiO_2 ETL. Even more relevant results the significantly improved photostability of the non-encapsulated $MAPbI_3$/C70 blend based ETL-free PSC with respect to the other two configurations examined, with a PCE still higher than 7% after 3 h of continuous illumination, whereas in the other cases devices were completely inactive after only 2 h.

4. Conclusions and Outlook

PSCs are currently driving change in non-conventional photovoltaics, with one of the steepest trends in performance growth over the last 40 years (Fig.1) [1]. Such an incomparable development has been made possible thanks to constant improvements in PVK materials quality, their processing and their interfacing with other established materials [118, 119] [22, 120-122]. Particularly, in this review we have stressed the very recent use of fullerene-based materials as ETLs in PSCs, both in standard and inverted architectures. In Fig. 15 we highlight the most important achievements obtained through the integration of fullerenes in PSCs until the publication of this review. However, the field is in continuous growth, so that during the writing many other works were published using fullerene derivatives as ETLs in PSCs.

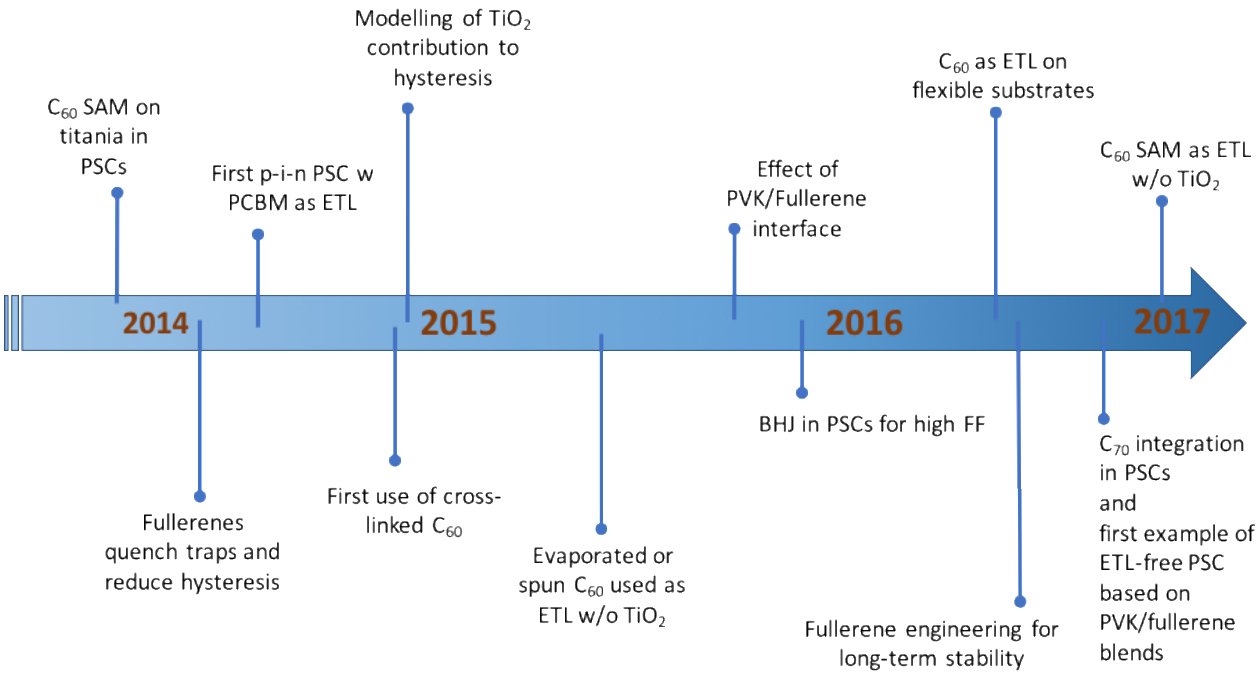

Fig. 16. The "milestones timeline" of fullerenes integration within PSCs.

The need for these molecular ETLs, with an already long track record built up within the OPV sector, has emerged following the first demonstration of their effectiveness in largely, or even completely, suppressing electrical hysteresis in PSCs [44]. Multiple efforts have been addressed in exploiting this peculiar ability of fullerene species. The field is evidently open to a large number of possible improvements and many people around the world are actively contributing to propose and test novel solutions for PSCs efficiency/stability growth making use of fullerene based ETLs.

The message coming from the first demonstrations [43, 44] has been perfectly accepted and allowed to flourish. Nevertheless, we believe a few guidelines for the further development of fullerene ETLs should be stated, which we have derived by thoroughly surveying the literature during the writing of this review. The key points that should be taken into account for the design, synthesis, preparation and characterization of novel fullerene-based ETLs for PSCs are the following:

1) The role of electron mobility within the fullerene ETL, that is intrinsically lower with respect to the one of PVKs, should be possibly understood and characterized at best. This property in fact largely influences the final FF, by affecting the series resistance, of the PSC. Chemical modification applied to the fullerene ETL can strongly influence the measured mobility, together with fullerene layer thickness. In BHJ PSC the difference in electron mobility between fullerene and PVK has to be properly considered for an optimized device engineering.
2) Fullerene ability to passivate PVK surface defects and its role as active component in BHJ PSCs is still under debate, although many researchers are arguing that fullerene molecules

have an action in limiting ion migration within the PVK layer, which is the main responsible for electrical hysteresis and, consequently device electrical stability: an extensive resume of the currently ongoing opinions on the subject is provided in the recently published perspective article from Huang et al. [67] nominated previously.

3) Energy levels of fullerene molecules are often reported, particularly LUMO levels, given the relevance they have for accepting electrons from PVK conduction bands. Unfortunately, they are often estimated from cyclic voltammetry measured in solution, where the fullerene molecules act as independent species, free to move in all possible directions, or from DFT calculations performed in vacuum. In order to gain more precise values, measurements or calculations should be done in the physical state which is closer to the one adopted by the ETL within the PSC, *i.e.* generally in thin film, this way taking into account the contribution to final energy levels coming from other surrounding species and physical constrains deriving from solid-state packing of molecules. Following this approach, reliable models can be developed, helpful for the determination of the PSC physics. Furthermore, the open circuit voltage of fullerene-based PSCs is largely determined by the quasi-Fermi level of the fullerene layer. This important aspect that deals with the energy order of fullerene molecules, has an impact on the possible use of doped fullerenes as ETLs. Therefore, when trying to integrate N-doped fullerenes in PSCs, researchers have to consider the possible advantages (the reduction of energy disorder, thus leading to higher Voc) and drawbacks (more interfacial recombination at the fullerene/PVK interface, i.e. lower Voc) as highlighted in Fig. 16 [123].
4) Fullerene molecules absorb visible light [124]. Therefore, layer thickness and optical transparency should be always evaluated in order to act positively on FF and Jsc, avoiding the unwanted reduction of light reaching the photoactive layer. This aspect has a tremendous impact on the development of tandem PVK/silicon tandem solar cells [125].
5) Hydrophobicity/hydrophilicity of the fullerene layer should be well assessed. This is often done by authors through contact angle measurements to furnish a reliable picture of surface polarity properties of the proposed fullerene ETL. On the other hand, as we have already discussed previously, the balance between hydrophobic and hydrophilic properties is not yet completely clarified for what concerns the use of fullerene ETLs in direct PSC architectures, with effects on PVK grain coarsening and PVK crystallinity, whereas in inverted architectures more hydrophobic layers might help in providing long-term stabilities because they can block moisture income.

6) Further structural characterizations of the fullerene ETLs might help in unraveling structure-property relationships and drive the design of improved ETLs. Thermal characterization (differential scanning calorimetry –DSC-, thermogravimetric analysis -TGA-) can provide precious information about the properties of materials in their as-deposited form and possible changes to which they can undergo when thermally treated (effects of annealing, determination of thermal stabilities). Crystallinity of fullerene films is also an important parameter which might deserve further attention and which can be derived, for instance, through X-ray analysis.

Inorganic ETLs are not completely UV stable and this issue is a real problem in PSCs containing titania-based ETLs [57]. Stability to UV irradiation should be tested in PSCs containing fullerene-based ETLs (when used in replacement of titania) to really prove that the material substitution is effective in addressing this problem and that the continuous illumination does not affect at the same time the fullerene chemical stability. Electron paramagnetic resonance has been recently applied to OPV for elucidating the role of photo-generated radicals in the deteriorating solar cell performances [60] and could be in perspective applied to fullerene containing PSCs to shine light on the possible existence of similar phenomena within these last ones as well.

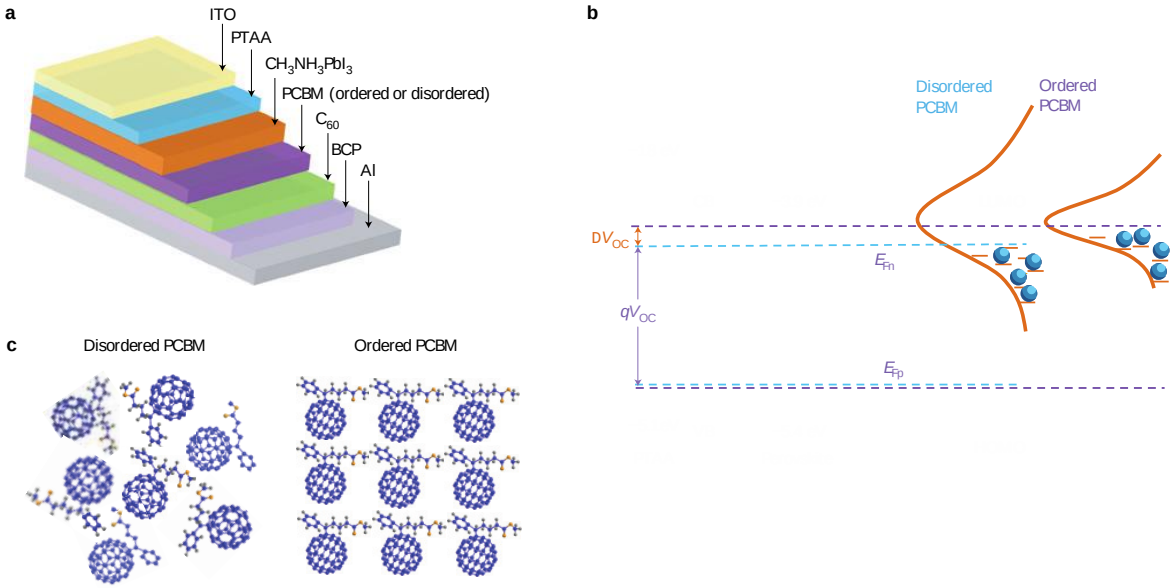

Fig. 17. Mechanism of Voc engineering aimed at reducing energy disorder. Reprinted from ref [123] with permission from Nature Publishing Group.

As received C_{60} and PCBM still dominate as the standard ETLs within fullerene containing PSCs proposed in the literature, because they can be used directly as they are provided from commercial sources, without the need for purifications or complex chemical modifications. Nevertheless, the

introduction of functional units on the fullerene scaffold has revealed a great potential in driving performance and stability of PSCs. Therefore, the testing of new derivatives, or simply the adoption of species which have demonstrated usefulness in other fields, might be one of the major directions to follow during the search for improvements in PSCs, which will finally lead to commercialization. The relevance of chemical approaches such as cross-linking, covalent immobilization and polarity control over fullerene derivatives has been highlighted in this review, providing the reader with a solid and critical knowledge of the fundamentals. The introduction of fullerene-based materials as the only ETLs within a PSC will likely simplify significantly the device production process, with large implications also in flexible electronics. At the same time anyway, it is required a great effort also in making easier and high-yielding the synthetic procedures needed to produce functionalized fullerene species. Continuous flow synthetic methods may represent a promising approach to allow for a safe and sustainable scale-up in the production of functionalized fullerenes, often requiring shorter times with respect to batch processes, as was already demonstrated for OPV applications [126, 127]. It is also true that the search for highly selective species, which can be used in small quantity to produce ultra-thin layers and in processes which implicate low material waist, might represent a major goal for researchers involved in the field. For this reason, chemical investigation should be always accompanied by studies on material's solid state assembly and suitable chemical modifications should also be supportive to the process. If coupled to more sophisticated analysis techniques for interfaces, able to really probe what takes place at the molecular level within this realm, which is profoundly different from the bulk of a material, research in this direction will certainly furnish crucial information for amplifying the control exerted on device quality and working mechanisms. As we said before, the sector is extremely dynamic and subjected to constant improvements. We believe that, together with representing a sort of "Renaissance" for fullerene molecules within basic research, large room is available for a fast entrance in the market of the fullerene-PVK technology.

Acknowledgements

Financial support from Centro Studi di Economia e Tecnica dell'Energia Giorgio Levi Cases of the University of Padova (project OPERA) is gratefully acknowledged.

References

[1] https://www.nrel.gov/pv/assets/images/efficiency-chart.png.
[2] A. Kojima, K. Teshima, Y. Shirai and T. Miyasaka, J. Amer. Chem. Soc. 131 (2009) 6050-6051.
[3] X. Li, D. Bi, C. Yi, J.-D. Décoppet, J. Luo, S. M. Zakeeruddin, A. Hagfeldt and M. Grätzel, Science (2016) 10.1126/science.aaf8060.
[4] https://www.weforum.org/agenda/2016/06/top-10-emerging-technologies-2016/
[5] M. Liu, M. B. Johnston and H. J. Snaith, Nature 501 (2013) 395-398.

[6] J. Burschka, N. Pellet, S.-J. Moon, R. Humphry-Baker, P. Gao, M. K. Nazeeruddin and M. Gratzel, Nature 499 (2013) 316-319.
[7] S. D. Stranks, G. E. Eperon, G. Grancini, C. Menelaou, M. J. P. Alcocer, T. Leijtens, L. M. Herz, A. Petrozza and H. J. Snaith, Science 342 (2013) 341-344.
[8] S. Collavini and J. L. Delgado, Adv. En. Mater. (2016) 1601000.
[9] R. Ganesamoorthy, G. Sathiyan and P. Sakthivel, Sol. Energ. Mat. Sol. Cells 161 (2017) 102-148.
[10] R. Po, M. Maggini and N. Camaioni, J. Phys. Chem. C 114 (2010) 695-706.
[11] B. C. Thompson and J. M. J. Fréchet, Angew. Chem. Int. Ed. 47 (2008) 58-77.
[12] A. Kuzmich, D. Padula, H. Ma and A. Troisi, En. Environ. Sci. 10 (2017) 395-401.
[13] Y. Lin and X. Zhan, Mater. Horiz. 1 (2014) 470-488.
[14] P. Sonar, J. P. Fong Lim and K. L. Chan, En. Environ. Sci. 4 (2011) 1558-1574.
[15] S. Li, Z. Zhang, M. Shi, C.-Z. Li and H. Chen, Phys. Chem. Chem. Phys. 19 (2017) 3440-3458.
[16] M. C. Scharber, D. Mühlbacher, M. Koppe, P. Denk, C. Waldauf, A. J. Heeger and C. J. Brabec, Adv. Mater. 18 (2006) 789-794.
[17] L. Echegoyen and L. E. Echegoyen, Acc. Chem. Res. 31 (1998) 593-601.
[18] A. Abrusci, S. D. Stranks, P. Docampo, H.-L. Yip, A. K. Y. Jen and H. J. Snaith, Nano Lett. 13 (2013) 3124-3128.
[19] S. Kongchao, S. Hao Liang, J. Gengwu, Y. Yingguo, J. Zheng and S. Fei, in *Nanoelectronics and Materials Development*, ed. A. Kar, Intech, 2016.
[20] N. Martín, Adv. Energy Mater. (2016) 1601102.
[21] A. Lekawa-Raus, J. Patmore, L. Kurzepa, J. Bulmer and K. Koziol, Adv. Funct. Mater. 24 (2014) 3661-3682.
[22] T. Gatti, S. Casaluci, M. Prato, M. Salerno, F. Di Stasio, A. Ansaldo, E. Menna, A. Di Carlo and F. Bonaccorso, Adv. Funct. Mater. 26 (2016) 7443-7453.
[23] A. L. Palma, L. Cinà, S. Pescetelli, A. Agresti, M. Raggio, R. Paolesse, F. Bonaccorso and A. Di Carlo, Nanoenergy 22 (2016) 349-360.
[24] A. Agresti, S. Pescetelli, B. Taheri, A. E. Del Rio Castillo, L. Cinà, F. Bonaccorso and A. Di Carlo, ChemSusChem 9 (2016) 2609-2619.
[25] J. T.-W. Wang, J. M. Ball, E. M. Barea, A. Abate, J. A. Alexander-Webber, J. Huang, M. Saliba, I. Mora-Sero, J. Bisquert, H. J. Snaith and R. J. Nicholas, Nano Lett. 14 (2014) 724-730.
[26] F. Langa and J.-F. Nierengarten, *Fullerenes: principles and applications*, RSC Publishing, 2007.
[27] G. Yu, J. Gao, J. C. Hummelen, F. Wudl and A. J. Heeger, Science 270 (1995) 1789-1791.
[28] A. J. Heeger, Adv. Mater. 26 (2014) 10-28.
[29] Y. Huang, E. J. Kramer, A. J. Heeger and G. C. Bazan, Chem. Rev. 114 (2014) 7006-7043.
[30] C. Cui, Y. Li and Y. Li, Adv. Energy Mater., DOI: 10.1002/aenm.201601251 (2016) 1601251.
[31] T. Liu and A. Troisi, Adv. Mater. 25 (2013) 1038-1041.
[32] S. K. Hau, Y.-J. Cheng, H.-L. Yip, Y. Zhang, H. Ma and A. K. Y. Jen, ACS Appl. Mater. Interfaces 2 (2010) 1892-1902.
[33] Y.-J. Cheng, F.-Y. Cao, W.-C. Lin, C.-H. Chen and C.-H. Hsieh, Chem. Mater. 23 (2011) 1512-1518.
[34] Y.-S. Cheng, S.-H. Liao, Y.-L. Li and S.-A. Chen, ACS Appl. Mater. Interfaces 5 (2013) 6665-6671.
[35] S. K. Hau, H.-L. Yip, H. Ma and A. K.-Y. Jen, Appl. Phys. Lett. 93 (2008) 233304.
[36] C. Luo, D. M. Guldi, M. Maggini, E. Menna, S. Mondini, N. A. Kotov and M. Prato, Angew. Chem. Int. Ed. 39 (2000) 3905-3909.
[37] C.-H. Hsieh, Y.-J. Cheng, P.-J. Li, C.-H. Chen, M. Dubosc, R.-M. Liang and C.-S. Hsu, J. Am. Chem. Soc. 132 (2010) 4887-4893.
[38] J. Li, F. Zhao, T. Wang, M. Nie, J. Li, Z. Wei, L. Jiang and C. Wang, J. Mater. Chem. A 5 (2017) 947-951.
[39] M. Wright and A. Uddin, Sol. Energ. Mat. Sol. Cells 107 (2012) 87-111.
[40] A. R. S. Kandada, S. Guarnera, F. Tassone, G. Lanzani and A. Petrozza, Adv. Funct. Mater. 24 (2014) 3094-3099.
[41] Y. Vaynzof, D. Kabra, L. Zhao, P. K. H. Ho, A. T.-S. Wee and R. H. Friend, Appl. Phys. Lett. 97 (2010) 033309.
[42] R. Nie, Y. Wang, W. Yuan, C. Chen and X. Deng, J. Phys. Chem. C 118 (2014) 18962-18968.

[43] Q. Wang, Y. Shao, Q. Dong, Z. Xiao, Y. Yuan and J. Huang, Energy Environ. Sci. 7 (2014) 2359-2365.
[44] K. Wojciechowski, S. D. Stranks, A. Abate, G. Sadoughi, A. Sadhanala, N. Kopidakis, G. Rumbles, C.-Z. Li, R. H. Friend, A. K. Y. Jen and H. J. Snaith, ACS Nano 8 (2014) 12701-12709.
[45] H. J. Snaith, A. Abate, J. M. Ball, G. E. Eperon, T. Leijtens, N. K. Noel, S. D. Stranks, J. T.-W. Wang, K. Wojciechowski and W. Zhang, J. Phys. Chem. Lett. 5 (2014) 1511-1515.
[46] Y. Shao, Z. Xiao, C. Bi, Y. Yuan and J. Huang, Nat. Commun. 5 (2014) 5784.
[47] Y. H. Chao, Y. Y. Huang, J. Y. Chang, S. H. Peng, W. Y. Tu, Y. J. Cheng, J. Hou and C. S. Hsu, J. Mater. Chem. A 3 (2015) 20382-20388.
[48] C. Tao, S. Neutzner, L. Colella, S. Marras, A. R. Srimath Kandada, M. Gandini, M. D. Bastiani, G. Pace, L. Manna, M. Caironi, C. Bertarelli and A. Petrozza, Energy Environ. Sci. 8 (2015) 2365-2370.
[49] P.-W. Liang, C.-C. Chueh, S. T. Williams and A. K. Y. Jen, Adv. Energy Mater. 5 (2015) 1402321.
[50] M. F. Lo, Z. Q. Guan, T. W. Ng, C. Y. Chan and C. S. Lee, Adv. Funct. Mater. 25 (2015) 1213-1218.
[51] Z. Xiao, Y. Yuan, Y. Shao, Q. Wang, Q. Dong, C. Bi, P. Sharma, A. Gruverman and J. Huang, Nat. Mater. 14 (2015) 193-198.
[52] M. De Bastiani, G. Dell'Erba, M. Gandini, V. D'Innocenzo, S. Neutzner, A. R. S. Kandada, G. Grancini, M. Binda, M. Prato, J. M. Ball, M. Caironi and A. Petrozza, (2016) 1501453.
[53] F. Lamberti, L. Litti, M. De Bastiani, R. Sorrentino, M. Gandini, M. Meneghetti and A. Petrozza, Adv. En. Mater. (2016) 1601703.
[54] J. Xu, A. Buin, A. H. Ip, W. Li, O. Voznyy, R. Comin, M. Yuan, S. Jeon, Z. Ning, J. J. McDowell, P. Kanjanaboos, J.-P. Sun, X. Lan, L. N. Quan, D. H. Kim, I. G. Hill, P. Maksymovych and E. H. Sargent, Nat. Commun. 6 (2015) 7081.
[55] Y. Li, Y. Zhao, Q. Chen, Y. Yang, Y. Liu, Z. Hong, Z. Liu, Y.-T. Hsieh, L. Meng, Y. Li and Y. Yang, J. Am. Chem. Soc. 137 (2015) 15540-15547.
[56] T. Leijtens, G. E. Eperon, S. Pathak, A. Abate, M. M. Lee and H. J. Snaith, Nat. Commun. 4 (2013) 2885.
[57] P. Topolovsek, F. Lamberti, T. Gatti, A. Cito, J. M. Ball, E. Menna, C. Gadermaier and A. Petrozza, J. Mater. Chem. A 5 (2017) 11882-11893.
[58] T. Heumueller, W. R. Mateker, A. Distler, U. F. Fritze, R. Cheacharoen, W. H. Nguyen, M. Biele, M. Salvador, M. von Delius, H.-J. Egelhaaf, M. D. McGehee and C. J. Brabec, En. Environ. Sci. 9 (2016) 247-256.
[59] N. Wang, X. Tong, Q. Burlingame, J. Yu and S. R. Forrest, Solar En. Mater. Solar Cells 125 (2014) 170-175.
[60] L. N. Inasaridze, A. I. Shames, I. V. Martynov, B. Li, A. V. Mumyatov, D. K. Susarova, E. A. Katz and P. A. Troshin, J. Mater. Chem. A 5 (2017) 8044-8050.
[61] C.-H. Chiang and C.-G. Wu, Nat. Photon. 10 (2016) 196-200.
[62] Y. Fang, C. Bi, D. Wang and J. Huang, ACS Energy Lett., DOI: 10.1021/acsenergylett.6b00657 (2017) 782-794.
[63] L. Shen, Y. Fang, D. Wang, Y. Bai, Y. Deng, M. Wang, Y. Lu and J. Huang, Adv. Mater. 28 (2016) 10794-10800.
[64] G. Paternò, A. J. Warren, J. Spencer, G. Evans, V. G. Sakai, J. Blumberger and F. Cacialli, J. Mater. Chem. C 1 (2013) 5619-5623.
[65] G. Tregnago, M. Wykes, G. M. Paternò, D. Beljonne and F. Cacialli, J. Phys. Chem. C 119 (2015) 11846-11851.
[66] K. Wang, C. Liu, P. Du, J. Zheng and X. Gong, Energy Environ. Sci. 8 (2015) 1245-1255.
[67] Y. Fang, C. Bi, D. Wang and J. Huang, ACS Energy Lett. 2 (2017) 782-794.
[68] C. S. Ponseca, E. M. Hutter, P. Piatkowski, B. Cohen, T. Pascher, A. Douhal, A. Yartsev, V. Sundström and T. J. Savenije, J. Amer. Chem. Soc. 137 (2015) 16043-16048.
[69] Y. Liu, M. Bag, L. A. Renna, Z. A. Page, P. Kim, T. Emrick, D. Venkataraman and T. P. Russell, Adv. En. Mater. 6 (2016) 1501606.
[70] J. Chang, J. Xiao, Z. Lin, H. Zhu, Q. H. Xu, K. Zeng, Y. Hao and J. Ouyang, J. Mater. Chem. A 4 (2016) 17464-17472.
[71] M. F. N. Taufique, S. M. Mortuza and S. Banerjee, J. Phys. Chem. C 120 (2016) 22426-22432.

[72] M. Valles-Pelarda, B. C. Hames, I. García-Benito, O. Almora, A. Molina-Ontoria, R. S. Sánchez, G. Garcia-Belmonte, N. Martín and I. Mora-Sero, J. Phys. Chem. Lett. 7 (2016) 4622-4628.
[73] H. S. Kim, I. H. Jang, N. Ahn, M. Choi, A. Guerrero, J. Bisquert and N. G. Park, 6 (2015) 4633-4639.
[74] W. Ke, D. Zhao, C. R. Grice, A. J. Cimaroli, J. Ge, H. Tao, H. Lei, G. Fang and Y. Yan, 3 (2015) 17971-17976.
[75] W. Ke, D. Zhao, C. R. Grice, A. J. Cimaroli, G. Fang and Y. Yan, J. Mater. Chem. A 3 (2015) 23888-23894.
[76] K. Wojciechowski, T. Leijtens, S. Siprova, C. Schlueter, M. T. Hörantner, J. T. W. Wang, C. Z. Li, A. K. Y. Jen, T. L. Lee and H. J. Snaith, 6 (2015) 2399-2405.
[77] D. Zhao, W. Ke, C. R. Grice, A. J. Cimaroli, X. Tan, M. Yang, R. W. Collins, H. Zhang, K. Zhu and Y. Yan, Nano En. 19 (2016) 88-97.
[78] S. Chang, G. D. Han, J. G. Weis, H. Park, O. Hentz, Z. Zhao, T. M. Swager and S. Gradečak, 8 (2016) 8511-8519.
[79] H. Yoon, S. M. Kang, J.-K. Lee and M. Choi, Energy Environ. Sci. 9 (2016) 2262-2266.
[80] K. Wojciechowski, I. Ramirez, T. Gorisse, O. Dautel, R. Dasari, N. Sakai, J. M. Hardigree, S. Song, S. Marder, M. Riede, G. Wantz and H. J. Snaith, ACS Energy Lett. 1 (2016) 648-653.
[81] W. Yan, S. M. Seifermann, P. Pierrat and S. Brase, Org. Biomol. Chem. 13 (2015) 25-54.
[82] T. M. Figueira-Duarte, J. Clifford, V. Amendola, A. Gegout, J. Olivier, F. Cardinali, M. Meneghetti, N. Armaroli and J.-F. Nierengarten, Chem. Commun. (2006) 2054-2056.
[83] Y. Nakamura and S.-I. Kato, Chem. Rec. 11 (2011) 77-94.
[84] A. Hirsch, Angew. Chem. Int. Ed. 32 (1993) 1138-1141.
[85] M. Durka, K. Buffet, J. Iehl, M. Holler, J.-F. Nierengarten, J. Taganna, J. Bouckaert and S. P. Vincent, Chem. Commun. 47 (2011) 1321-1323.
[86] E. Nakamura and H. Isobe, Acc. Chem. Res. 36 (2003) 807-815.
[87] Y.-Y. Huang, S. K. Sharma, R. Yin, T. Agrawal, L. Y. Chiang and M. R. Hamblin, J. Biomed. Nanotechnol. 10 (2014) 1918-1936.
[88] A. Dellinger, Z. Zhou, J. Connor, A. B. Madhankumar, S. Pamujula, C. M. Sayes and C. L. Kepley, Nanomedicine 8 (2013) 1191-1208.
[89] M. Cristofani, E. Menna, M. Seri, M. Muccini, M. Prosa, S. Antonello, M. Mba, L. Franco and M. Maggini, Asian J. Org. Chem. 5 (2016) 676-684.
[90] L. Chen, K. Yao and Y. Chen, J. Mater. Chem. 22 (2012) 18768-18771.
[91] R. Maria Giron, J. Marco-Martinez, S. Bellani, A. Insuasty, H. Comas Rojas, G. Tullii, M. R. Antognazza, S. Filippone and N. Martin, J. Mater. Chem. A 4 (2016) 14284-14290.
[92] P. Salice, M. Mauri, M. Castellino, M. De Marco, A. Bianchi, A. Virga, A. Tagliaferro, R. Simonutti and E. Menna, Chem. Commun. 49 (2013) 8048-8050.
[93] P. Innocenzi, P. Falcaro, S. Schergna, M. Maggini, E. Menna, H. Amenitsch, J. A. A. Soler-Illia, D. Grosso and C. Sanchez, J. Mater. Chem. 14 (2004) 1838-1842.
[94] A. Cravino, G. Zerza, H. Neugebauer, S. Bucella, M. Maggini, E. Menna, G. Scorrano, M. Svensson, M. R. Andersson and N. S. Sariciftci, Synth. Met. 121 (2001) 1555-1556.
[95] H. Azimi, T. Ameri, H. Zhang, Y. Hou, C. O. R. Quiroz, J. Min, M. Hu, Z. G. Zhang, T. Przybilla, G. J. Matt, E. Spiecker, Y. Li and C. J. Brabec, Adv. En. Mater. 5 (2015) 1401692.
[96] Q. Xu, Z. Lu, L. Zhu, C. Kou, Y. Liu, C. Li, Q. Meng, W. Li and Z. Bo, J. Mater. Chem. A 4 (2016) 17649-17654.
[97] T. Cao, Z. Wang, Y. Xia, B. Song, Y. Zhou, N. Chen and Y. Li, ACS Appl. Mater. Interfaces 8 (2016) 18284-18291.
[98] W. Zhou, J. Zhen, Q. Liu, Z. Fang, D. Li, P. Zhou, T. Chen and S. Yang, J. Mater. Chem. A 5 (2017) 1724-1733.
[99] C. Tao, J. Van Der Velden, L. Cabau, N. F. Montcada, S. Neutzner, A. R. Srimath Kandada, S. Marras, L. Brambilla, M. Tommasini, W. Xu, R. Sorrentino, A. Perinot, M. Caironi, C. Bertarelli, E. Palomares and A. Petrozza, Adv. Mater., DOI: 10.1002/adma.201604493 (2017) 1604493.
[100] B. L. Watson, N. Rolston, K. A. Bush, T. Leijtens, M. D. McGehee and R. H. Dauskardt, ACS Appl. Mater. Interfaces 8 (2016) 25896-25904.

[101] S. Shao, M. Abdu-Aguye, L. Qiu, L. H. Lai, J. Liu, S. Adjokatse, F. Jahani, M. E. Kamminga, G. H. Ten Brink, T. T. M. Palstra, B. J. Kooi, J. C. Hummelen and M. Antonietta Loi, 9 (2016) 2444-2452.
[102] Y. Bai, Q. Dong, Y. Shao, Y. Deng, Q. Wang, L. Shen, D. Wang, W. Wei and J. Huang, Nat. Commun. 7 (2016) 12806.
[103] C.-B. Tian, K. Kochiss, E. Castro, G. Betancourt-Solis, H. Han and L. Echegoyen, J. Mater. Chem. A 5 (2017) 7326-7332.
[104] F. Zhang, W. Shi, J. Luo, N. Pellet, C. Yi, X. Li, X. Zhao, T. J. S. Dennis, X. Li, S. Wang, Y. Xiao, S. M. Zakeeruddin, D. Bi and M. Grätzel, Adv. Mater. (2017) 1606806.
[105] R. Sandoval-Torrientes, J. Pascual, I. García-Benito, S. Collavini, I. Kosta, R. Tena-Zaera, N. Martín and J. L. Delgado, ChemSusChem 10 (2017) 2023-2029.
[106] S. Collavini, I. Kosta, S. F. Völker, G. Cabanero, H. J. Grande, R. Tena-Zaera and J. L. Delgado, ChemSusChem, DOI: 10.1002/cssc.201600051 (2016) 1263-1270.
[107] Z.-G. Zhang, H. Li, B. Qi, D. Chi, Z. Jin, Z. Qi, J. Hou, Y. Li and J. Wang, J. Mater. Chem. A 1 (2013) 9624-9629.
[108] N. Deb, R. R. Dasari, K. Moudgil, J. L. Hernandez, S. R. Marder, Y. Sun, A. Karim and D. G. Bucknall, J. Mater. Chem. A 3 (2015) 21856-21863.
[109] D. Bi, W. Tress, M. I. Dar, P. Gao, J. Luo, C. Renevier, K. Schenk, A. Abate, F. Giordano, J.-P. Correa Baena, J.-D. Decoppet, S. M. Zakeeruddin, M. K. Nazeeruddin, M. Grätzel and A. Hagfeldt, Sci. Adv. 2 (2016) e1501170.
[110] M. Maggini, C. De Faveri, G. Scorrano, M. Prato, G. Brusatin, M. Guglielmi, M. Meneghetti, R. Signorini and R. Bozio, Chem. Eur. J. 5 (1999) 2501-2510.
[111] K. Leo, Nat. Nanotech. 10 (2015) 574-575.
[112] T. A. Berhe, W.-N. Su, C.-H. Chen, C.-J. Pan, J.-H. Cheng, H.-M. Chen, M.-C. Tsai, L.-Y. Chen, A. A. Dubale and B.-J. Hwang, Energy Environ. Sci. 9 (2016) 323-356.
[113] T. Leijtens, G. E. Eperon, N. K. Noel, S. N. Habisreutinger, A. Petrozza and H. J. Snaith, Adv. Energy Mater. 5 (2015) 1500963.
[114] S. D. Stranks, V. M. Burlakov, T. Leijtens, J. M. Ball, A. Goriely and H. J. Snaith, Phys. Rev. Appl. 2 (2014) 034007.
[115] C. Zhao, B. Chen, X. Qiao, L. Luan, K. Lu and B. Hu, Adv. En. Mater. 5 (2015) 1500279.
[116] S. M. Dai, H. R. Tian, M. L. Zhang, Z. Xing, L. Y. Wang, X. Wang, T. Wang, L. L. Deng, S. Y. Xie, R. B. Huang and L. S. Zheng, J. Power Sources 339 (2017) 27-32.
[117] J. Pascual, I. Kosta, T. Tuyen Ngo, A. Chuvilin, G. Cabanero, H. J. Grande, E. M. Barea, I. Mora-Seró, J. L. Delgado and R. Tena-Zaera, ChemSusChem 9 (2016) 2679-2685.
[118] L. Calió, S. Kazim, M. Grätzel and S. Ahmad, Angew. Chem. Int. Ed. 55 (2016) 14522-14545.
[119] G. Yang, H. Tao, P. Qin, W. Ke and G. Fang, J. Mater. Chem. A 4 (2016) 3970-3990.
[120] Y. Rong, L. Liu, A. Mei, X. Li and H. Han, Adv. Energy Mater. 5 (2015) 1501066.
[121] F. Matteocci, L. Cinà, E. Lamanna, S. Cacovich, G. Divitini, P. A. Midgley, C. Ducati and A. Di Carlo, Nanoenergy 30 (2016) 162-172.
[122] B. Li, Y. Li, C. Zheng, D. Gao and W. Huang, RSC Adv. 6 (2016) 38079-38091.
[123] Y. Shao, Y. Yuan and J. Huang, Nat. Energy 1 (2016) 15001.
[124] G. Brusatin and R. Signorini, J. Mater. Chem. 12 (2002) 1964-1977.
[125] B. Chen, X. Zheng, Y. Bai, N. P. Padture and J. Huang, Adv. En. Mater. (2017) 1602400.
[126] H. Seyler, W. W. H. Wong, D. J. Jones and A. B. Holmes, J. Org. Chem. 76 (2011) 3551-3556.
[127] E. Rossi, T. Carofiglio, A. Venturi, A. Ndobe, M. Muccini and M. Maggini, Energy Environ. Sci. 4 (2011) 725-727.

Vitae

Teresa Gatti received her PhD degree in Materials Engineering from Politecnico di Milano in March 2014. Since September 2014 is a post-doctoral fellow in the group of Prof. Enzo Menna at the Department of Chemical Sciences of the University of Padova. She works on the chemical functionalization of carbon nanomaterials for the obtainment of advanced nanocomposites. These are mainly designed for use as functional materials in energy-related applications.

Enzo Menna is Associate Professor of Organic Chemistry at the University of Padova where he received his PhD degree in Chemistry in 1999 with a project concerning the study of hydrogen bonds by NMR measurements and quantum chemical calculations. His present activity concerns the synthesis of organic materials. Since 1999 he has studied the chemistry of carbon nanotubes, an almost unexplored topic at that time, then extended to other carbon nanostructures (CNS). His research is focused on the synthesis of soluble and functional CNS derivatives and their incorporation in polymer composites, to obtain materials for energy conversion and biomedical applications.

Moreno Meneghetti is a Full Professor of Physical Chemistry since 2002 and head of the Nanostructures and Optics Laboratory. His current research interest is focused on the synthesis of nanostructures for solar energy conversion and for nanomedicine applications. He contributed to develop a new synthesis based on the laser ablation of materials in solution and to a new approach for the calculations of the optical properties of correlated low dimensional systems.

Michele Maggini is Full Professor of Organic Chemistry at the University of Padova since 2000. His current research interests focus mainly on the functionalisation of carbon nanostructures for solar energy conversion and on the development of flow chemistry platforms for the synthesis of functionalized nanosystems and active pharmaceutical ingredients - www.chimica.unipd.it/michele.maggini

Annamaria Petrozza was awarded a Master of Science in Electronic Engineering at Ecole Supèrieure d'Electricité (Paris, France) in 2003 and at Politecnico of Milan in 2004 under the T.I.M.E. (Top Industrial Manager in Europe) program. In 2009 she received her PhD in Physics from the University of Cambridge (UK. From July 2008 to December 2009 she worked as research scientist at the Sharp Laboratories of Europe, Ltd on the development of new market competitive solar cell technologies. In January 2010, she moved to Istituto Italiano di Tecnologia where she is actually holding a Tenure Track Scientist position. Her research work mainly aims to shed light on interfacial optoelectronic mechanisms with the goal of improving efficiency and stability of solution processable semiconductors and devices, with special emphasis on highly efficient third generation solar cells.

Francesco Lamberti obtained his PhD degree in Material Sciences and Engineering from the University of Padova in 2011. After studying electrochemical biosensors on optically transparent electrodes, he moved to the Italian Institute of Technology (IIT) in Milano, working in the group of Dr. Annamaria Petrozza on the development of perovskite solar cells. Currently, he holds a senior post-doc position at the University of Padova granted by Fondazione Levi Cases on the preparation and study of nano-materials for perovskite solar cells exploiting laser ablation assisted in solution technique.